Competition sensitive! Draft of 2022.03.06–17:32

Augmenting Lunar Laser Ranging observations with Very Long Baseline Interferometry

Submitted in response to Research Opportunities in Space and Earth Sciences (ROSES) — 2021 Solicitation: NNH21ZDA001N-PDART, program C.4 Planetary Data Archiving, Restoration, and Tools

Contents

1 Executive Summary

Returning to the Moon in the coming years will provide an increasing number of opportunities to use telemetry signals from landers as radio beacons for precise geodesy on the Moon. We will develop, validate, and publicly release a tool, PlaVDA (Planetary VLBI Data Analysis), to process Level 1 Very Long Baseline Interferometry (VLBI) observations of lunar landers into a form that can be used by the planetary community for science analysis. Without such a tool, processing Level 1 VLBI data requires deep knowledge of VLBI techniques that most planetary scientists do not have. PlaVDA will remove barriers and allow new investigations utilizing artificial radio sources placed on the Moon that will provide new data on lunar geophysics for a very low cost without development of a dedicated payload.

Availability of Level 2 VLBI data products will allow to independently check and validate scientific results of Lunar Laser Range (LLR) observations of retroreflectors delivered to the Moon by prior missions. This is crucial as they are a cornerstone of lunar geophysics.

2 Introduction

In the 20th century geodesy evolved from a utilitarian technique for measuring land plots to a foundation of navigation and an environmental science. The Earth's surface is static at scales up to several decades at a level of accuracy coarser than tens meters. Measurements with a 1 meter accuracy detect large earthquakes and polar motion. Measurements with the of accuracy of 10 cm level detect solid tides and plate tectonics on scales of decades. Measurements at a sub-centimeter level of accuracy reveal the presence of the liquid core, crustal deformation caused by air and ocean mass re-distribution, and they allow to constrain parameters of the visco-elastic response of the mantle and physical properties of the core.

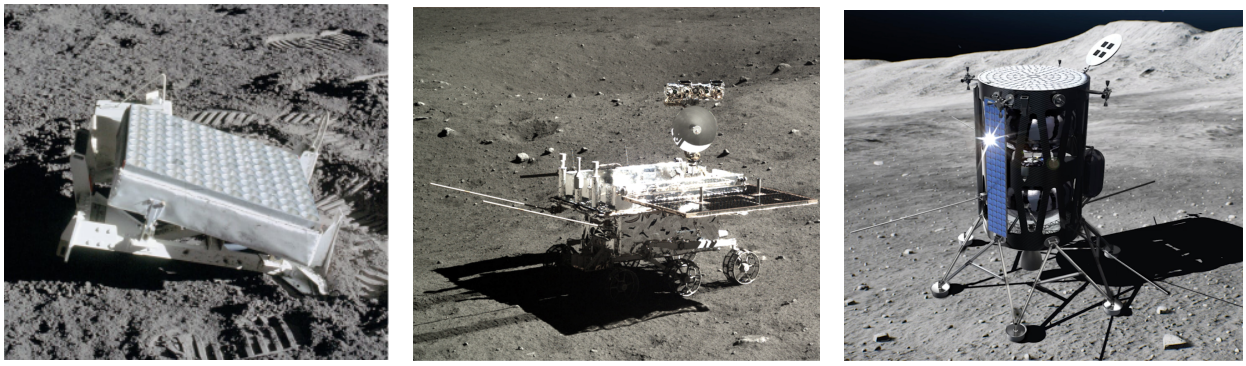

Figure 1: Instruments for selenodesy. *Left:* retroreflector installed by Apollo–11 mission operating since 1969. *Center:* radio beacon at Chang'E3 operating in 2015–2016. *Right:* radio beacon at LN-1 to be launched in 2022.

Geodetic observations on the Moon's surface have a similar potential to reveal the dynamics of the Moon's crust. The absence of air and water on the Moon facilitates interpretation of crust displacements and irregularities in the Moon's rotation. The era of selenodesy started in 1969 with a placement of the first retroreflector on the Moon during NASA Apollo-11 mission (Bender et al., 1973; Dickey et al., 1994). By now, there are 5 retroreflectors that form the fundamental selenodesy network. These retroreflectors are observed from the Earth's using the LLR

technique (Currie et al., 2011; Murphy et al., 2012; Murphy, 2013) that determines the travel time between a ground station and a retroreflector with a sub-centimeter level of accuracy.

These observations were used for improvement of the Lunar orbit determination (Folkner et al., 1994; Chapront et al., 2002; Williams et al., 2014; Williams and Boggs, 2016), for estimation of the Moon rotation parameters called physical librations (Pavlov et al., 2016; Dumberry and Wieczorek, 2016), for determination of the Lunar crust displacements caused by tides (Williams and Boggs, 2015; Pavlov, 2020), study of the Lunar core and its parameters (Meyer and Wisdom, 2011; Viswanathan et al., 2019), and for testing fundamental physics theories (Turyshev et al., 2012; Williams et al., 2012; Hofmann and Müller, 2018). Analysis of lunar solid tides that reach $\pm$ 9 cm provides information on dissipation in the Moon's mantle at time scales that have not been probed by laboratory experiments and are only starting to be explored for the Earth (Matsumoto et al., 2015; Matsuyama et al., 2016; Harada et al., 2016). LLR first demonstrated that the Moon has a fluid core by detecting the energy dissipated by the flow of the fluid along the core mantle boundary from analysis of irregularities in Moon's rotation (Williams et al., 2001).

However, LLR has its own weakness. Observing from the Earth an array of five retroreflectors on the near side of the Moon, always facing the Earth, makes separations of variables that describe the Moon's orbital motion, rotation, and tides problematic. This results in large correlations between estimates, which makes interpretation of results difficult and less certain. Planned placements of new retroreflectors in future missions is expected to mitigate this problem to some extent, but will not eliminate it. The root of the problem is that the retroreflectors see the Earth always at an angle that varies by only a few degrees (See Figure 2), while the coverage in a range of $\pm 180^\circ$ is optimal for variable separation.

The only other technique that is sensitive to Moon's orbital motion, rotation, and deformation is VLBI. A network of radiotelescopes synchronously observes a radio-beacon or a natural extragalactic source such as active galactic nucleus (AGN). The data acquisition system of ground stations digitizes the voltage of the received emission, records it on disk, and inserts time stamps from an ultra-stable atomic clock. The first stage of the data analysis computes the Level 1 data product: time series of spectra of cross- and auto-correlation functions of recorded voltage. Time delay of the wavefront arrival to station #2 with respect to station #1 with an accuracy < 1 cm is derived from processing these time series (See Figure 2). The power of the VLBI technique for application to planetary sciences comes from its ability to process the emission from both artificial beacons and natural radio sources, such as AGNs. Analysis of such observations allows us to determine the angular displacement of the radio beacon with respect to an AGN direction. Since AGNs are located at gigaparsec distances (1 gigaparsec $\approx 3 \cdot 10^{22}$ meter), a coordinate system based on AGNs is inertial. **Therefore, differential VLBI observations anchor the instantaneous lander position to the inertial space.** Selecting an AGN at a small angular distance from the Moon allows to mitigate errors of modeling the atmospheric path delay approximately by a factor of the angular distance between an AGN and the beacon expressed in radians.

3 Motivation and problem statement

Although the potential of VLBI observations for planetary science was realized five decades ago (Counselman et al., 1973), progress was slow due to difficulties with data analysis. The VLBI technique is commonly used for geodesy, for imaging of continuum spectrum sources such as AGNs, and for differential astrometry between two continuum spectrum source or between a

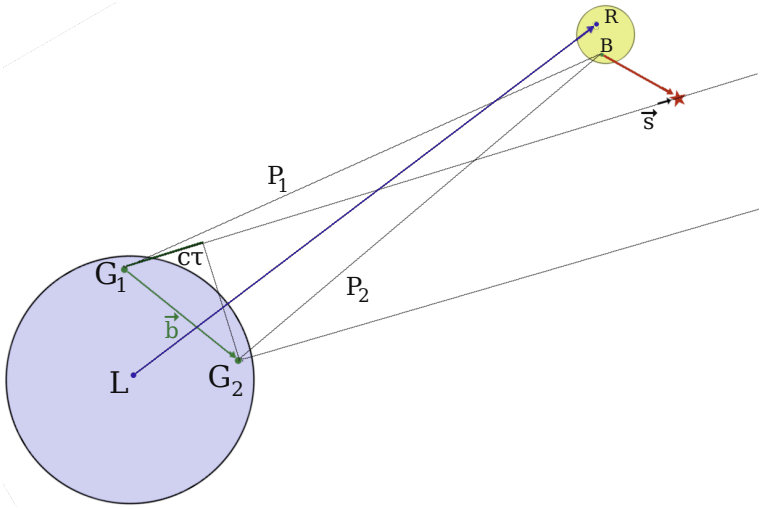

Figure 2: Geometry of VLBI observations. Baseline vector $\vec{b}$ connects two ground stations G_1 and G_2. The unit vector of the extragalactic source position is denoted with $\vec{s}$. VLBI evaluates path delay $c\tau = |P_1| - |P_2|$ from the satellite and $c\tau = \vec{b} \cdot \vec{s}$ from a background extragalactic radio source. Differential observations of both lunar lander B and the source S allow us to determine precisely the vector between them that is almost **orthogonal** to the line of sight. LLR determines the length between the ground station L and the retroreflector R **along** the line of sight.

continuum source and a narrow-band source, such as a stellar maser.

We will develop the methodology for processing of differential VLBI observations of Lunar landers and AGNs to derive the most precise lander position. Phase referencing VLBI was successfully used for locating slow-moving interplanetary spacecrafts (Fomalont et al., 2010; Duev et al., 2012; Park et al., 2015; Jones et al., 2020), however its use for observations of a Lunar lander that moves quickly over the sky poses an additional challenge and it has not been explored before. The principal difficulty is that the motion of a lander with respect to the inertial space is not known precisely before its positions are determined. The problem can be resolved, but it requires a large number of extra steps. Based on the methodology outlined below, we will develop a tool that processes VLBI observations and generates a) time series of differential phases between a lander and an AGN, as well as their rate of change and b) time series of angular position offsets of the lander with respect to background AGNs.

According to Reid and Honma (2014); Deller et al. (2019), precision of differential VLBI for measuring the angular distance between a target and a calibrator is at a level of 20–40 μas, or 3–6 cm at the Moon surface. The accuracy of derived lander coordinates is limited by errors of AGN positions that are at a level of 100 μas or 15 cm. Since the Moon is moving over the celestial sphere, many calibrators will be observed while the Moon passes nearby, and therefore, the impact of calibrator position errors on lander position estimates will be diminished. Therefore, a campaign of 10–100 observing sessions 8–20 hour long each has a potential to determine lander position on the Moon with the accuracy comparable with the accuracy of the LLR technique.

VLBI differential phase referencing data have a significant impact in the field of Lunar sciences for the following reasons. VLBI data are independent of LLR. When analyzed separately, analysis of discrepancies can be used for LLR validation. Second, LLR and differential VLBI observables are sensitive to mutually orthogonal projections of instantaneous lander position and

therefore, when analyzed together, synergism will be achieved, because a combined use of orthogonal observables improves variable separation and improves robustness of results. For instance, VLBI ties the lander position and therefore, the Moon's orbit, directly to the inertial coordinate system based on extragalactic objects. Therefore, systematic errors in Moon's orbit derived from LLR alone will be mitigated. Third, VLBI allows to get more dense time series, 200–2000 phase delays and rates points per an observing session within a given day, independent on weather, compare with 10–30 normal points per clear sky night from LLR observations.

The major motivation of our work is to lift barriers that impede proliferation of VLBI observations of spacecrafts on the Moon.

4 Methodology

VLBI observations of artificial signals from planetary landers can be done in three modes: a) phase tracking (Kikuchi et al., 2004; Sun et al., 2018; He et al., 2017; Liu et al., 2020), b) geodetic mode using group delays (ΔDOR) (Kikuchi et al., 2004; James et al., 2009), and c) phase referencing mode (Jones et al., 2020). Fluctuations of the path delay in the atmosphere limit the accuracy of observations in the first two modes to several meters on the Moon. Observations in the phase referencing modes allow to reduce of the impact of the atmosphere by more than one order of magnitude.

Phase-referencing is the main technique in radio astronomy that is de facto a default mode. A scheme of these is shown in Figure 2. Observations are made in a sequence C-T-C-T- ... . All antennas of the array dwell on a phase calibrator (C) then slew to a target (T), then back, etc. The period of time antennas collect the data is called a scan. A typical scan duration is 15–150 s. Calibrators are selected within 1–3° of a target (Martí-Vidal et al., 2010). Since the Moon is moving with respect to the inertial space with a rate of approximately 30′ per hour, the angular distance of a beacon with respect to calibrators is evolving. The network of observing stations is changing when the Moon is setting at some stations and rising at others. Therefore, observations are organized with blocks of 30–50 minutes long. Neighboring blocks may thus have different stations and/or different calibrators.

The primary goal of this project is to develop an algorithm for processing phase referencing observations of a Lunar lander and evaluate a position offset of the lander with respect to natural extragalactic radio sources used as calibrators. The data analysis procedure has a number of steps, and each step is refining the previous results.

4.1 Correlation

Digitized voltage records from the ground station receivers are processed with the so-called software correlator, program DiFX (Deller et al., 2007, 2011) supported by the radio astronomy community. This software will be directly used for processing data from calibrators. It will be slightly upgraded to perform precise computation of path delay from the lander. Since the extragalactic source is located in the far field zone, and path delay is computed assuming the wavefront is parallel (Kopeikin and Schäfer, 1999). That approach is not applicable for processing observations of an object in the near field zone. **We will develop program difx_nz for computation of path delay for the beacon with selenocentric a priori position $\vec{B}$ observed from ground stations G_1 and G_2 at the moment t_1 of the arrival of the wavefront to G_1. We will be using the semi-analytical approach that we have developed in the past (Jaron and Nothnagel, 2018).**

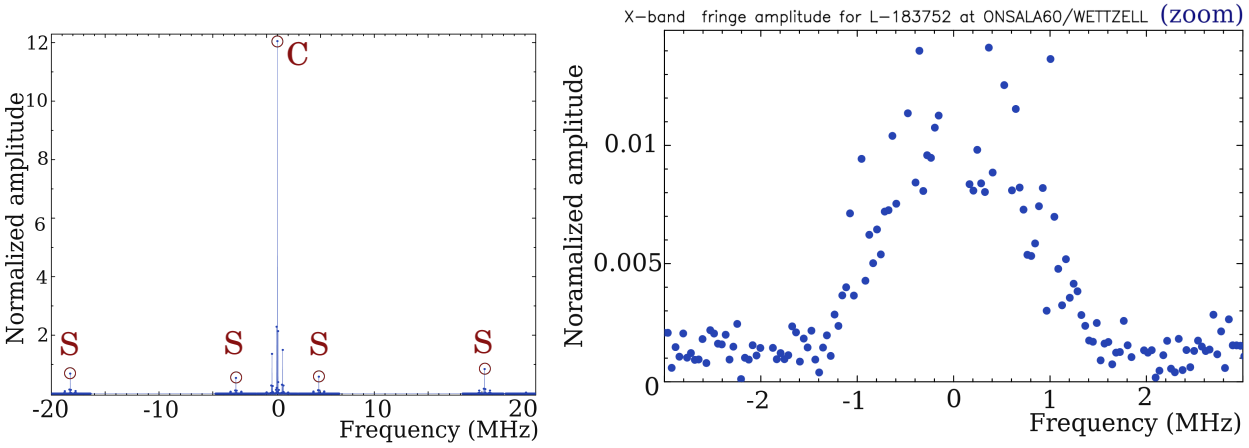

Figure 3: *Left* Amplitude spectrum of the the signal from Chang'E3 lander within 20 MHz bandwidth centered at 8.47 GHz. Letter **C** denotes the carrier and letters **S** denote sidelobes. *Right:* zoom of the spectrum near the signal carrier. This plots does not show a number of narrow-band spectral constituents that are beyond the plotting area.

The correlation is performed with some initial coarse path delay model. **We will develop software for preprocessing the raw output of the time series of the cross-correlation spectrum also known as visibilities. This will include computation of corrections to the difference $\Delta\tau$ between a precise path delay computed as described above and the one used as a priori during correlation, correcting the visibilities, then splitting the data into observations of the lander and calibrator sources, performing an initial quality control, and storing the updated dataset.**

The principal difficulty in processing of lander observations is that the lander is moving with respect to the inertial system because of Moon's orbital motion and rotation. Applying the a priori Moon's and a priori lander position reduces the residual motion but does not fully eliminates it. In order to reach the target accuracy, visibility data should be accumulated and *coherently* averaged. Coherent averaging requires the phases be stable within the averaging interval. That requires a knowledge of the improved lander position. This is a non-linear problem, specific to the planetary VLBI observations, and it is solved with iterations. The solution we propose is outlined below.

4.2 Processing group delays

Figure 3 shows the spectrum of the Chang'E3 lander which is typical. The signal consists of a narrow-band carrier, a number of additional narrow-band tones, and the broad-band constituent with the spectrum shape close to the Gaussian function. The width of the emitted narrow-band tones varies within 0.01–100 Hz depending on the emitter hardware, and the tones are spread over 10–100 MHz. The broad-band signal has the width of about 1 MHz and is associated with a telemetry channel. These constituents are processed separately.

First, the observations of calibrator sources are processed in usual way of analysis of continuum spectrum objects (Petrov, 2021). During that stage, phase delay τ_p, phase delay rate $\dot{\tau}_p$, and group delay τ_g are adjusted using the cross-correlation time series of a given scan in such a way that the coherent sum C of complex cross-correlation samples c_{kj}

$$C(\tau_p,\tau_g,\dot{\tau}_p) = \sum_k \sum_j c_{kj}\, e^{i(\omega_0\tau_p + \omega_0\dot{\tau}_p(t_k-t_0) + (\omega_j-\omega_0)\tau_g)} \qquad (1)$$

reaches the maximum amplitude. Index k runs over time, and index j runs over frequencies. ω_0 and t_0 denote the reference circular frequency within the band and the reference time within a scan, ω_j is the subband frequency. See Figure 4(left) for an illustration of phase and group delays. Then using estimates of group delays and phase delay rates, the visibilities are averaged over time and frequency with the specified averaging intervals. The averaged visibilities are later used for reconstruction of radio-images of phase calibrators in a form of two-dimensional brightness distributions $B(x,y)$.

Second, broad-band group delay from lander observations is computed using a portion of the spectrum with the lander broad-band signal by maximizing amplitude of $C(\tau_p, \tau_g, \dot{\tau}_p)$ in Eq. 1 using the common fringe fitting procedure (Petrov et al., 2011a). Since the bandwidth of the lander broad-band spectrum is usually narrower than the recorded bandwidth, the spectrum is multiplied by a mask that consists of 0 and 1 to limit the dataset with the data that contains the signal from the lander. If the lander spectrum is not a priori known, the procedure for bandwidth determination based on analysis of autocorrelation runs. This procedure computes the noise level in the frequency band where no signal is expected and finds the portion of the auto-spectrum that deviates by N times of the root mean square of the noise.

Broad-band group delays from observations of calibrators and the lander are processed in the same fashion as in geodetic VLBI analysis. The correction to the a priori selenocentric lander position, as well as nuisance parameters, such as the atmospheric path delay in the zenith direction at observing stations, and clock biases are adjusted using group delays. Depending on the design of observations and the spectrum of the emitted signal, the position accuracy of a Lunar lander determined that way ranges from 10 to 1000 meters. The adjusted parameters form the basis for further refinements.

These blocks of the computational procedures are already developed and they are used for processing routine geodetic and astronomical observations. We propose the following work: a) to upgrade existing software for path delay computation to support a planetary lander; b) to develop software that executes the computational blocks within a pipeline that combines observations of calibrators and the lander; c) to develop a database that would hold intermediate results of these computations; and d) to develop quality control procedures that would determine outliers in lander observations and flag bad data.

4.3 Processing phase delays and delay rates

A lander has a narrow band signal near the carrier (See Figure 3(left)). Determination of the phase of this signal is the goal of this stage of data analysis. Phase delays are a factor of 10–100 more precise than group delays, but have ambiguities with spacings c/f that are 3.5 cm for Chang'E3 observations.

The frequency of the carrier signal is changing in time. Its time evolution has a regular constituent due to the Doppler shift and a jitter due to the instability of the on-board frequency standard. The a priori model used for correlation subtracts the known part of the Doppler shift, but it retains the residual Doppler shift due to an uncertainty in lander position. Because of these factors, the spectrum of the carrier broadens (See Figure 4 (right)).

We will filter out the part of the spectrum that contains the signal from the carrier within $[\omega_o - \omega_b, \omega_o + \omega_b]$ frequency range, where ω_o is the frequency of the maximum. If the model were perfect and the lander frequency oscillator had no jitter, the interferometer response, i.e. the

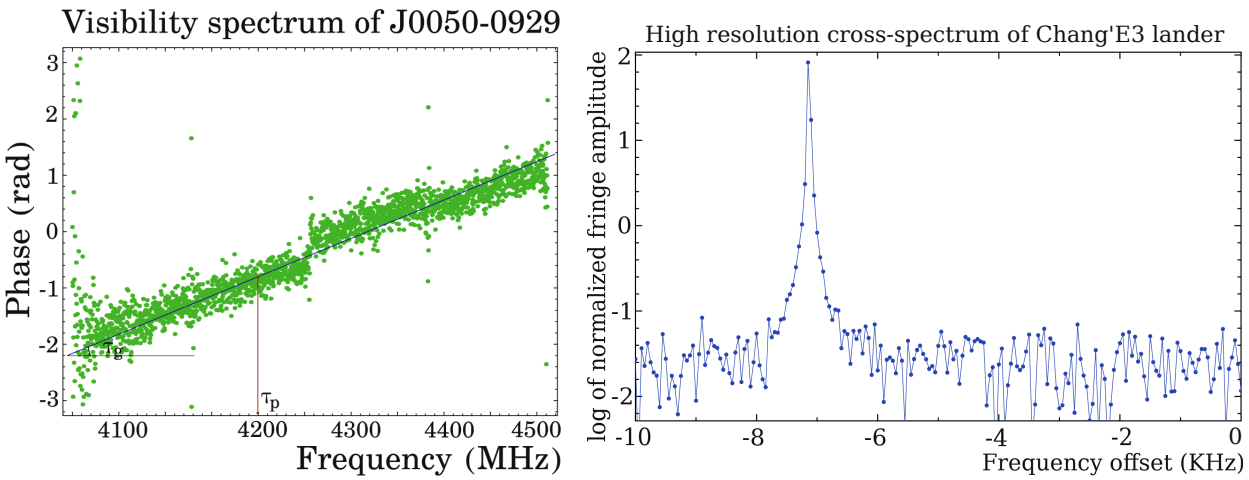

Figure 4: *Left:* Example of the dependence of visibility phase φ on frequency. Group delay is defined as $\tau_g = \dfrac{\partial\varphi}{\partial\omega}$, while phase delay at the reference cyclic frequency ω_0 is defined as $\tau_p = \dfrac{\varphi}{\omega_0}$. *Right:* Logarithm of visibility amplitudes of the Chang'E3 versus frequency centered at 8.47 GHz with a resolution of 50 Hz. The spectrum of the carrier is broadened because of the frequency jitter and unaccounted residual lander motion in the inertial space.

inverse Fourier transform of the cross-spectrum $C(t,\omega)$, would be $\cos(\omega_0\tau_p)$. We represent the inverse Fourier transform of the cross-spectrum $\mathcal{F}^{-1}(C(t,\omega))$ as

$$\mathcal{F}^{-1}(C(t,\omega)) = A\cos\left(\omega_0\cdot\left(1+\sum b_i B_i^k(t)\right)\cdot\left(\tau_p+(t-t_0)\dot{\tau}_p+\frac{1}{2}(t-t_0)^2\ddot{\tau}_p\right)\right), \qquad (2)$$

where $B_i^k(x)$ is the basis spline of the kth degree. We will fit b_i, τ_p, $\dot{\tau}_p$, $\ddot{\tau}_p$ using the inverse Fourier transform of the time series of the cross-spectra of a given scan within the frequency range $[\omega_o-\omega_b,\omega_o+\omega_b]$. We will perform a non-linear least squares fit using initial values of τ_p and $\dot{\tau}_p$ determined at the previous step of data analysis. Initial values of b_i will be evaluated using visibility amplitudes. We will use unambiguous $\dot{\tau}_p$ and $\ddot{\tau}_p$ collected from all the scans to further refine the lander position, and then we will re-compute group delays and repeat computation of phase delays with the updated a priori lander position.

We will develop new software for these steps. That will include detection of the carrier within $[\omega_o-\omega_b,\omega_o+\omega_b]$ frequency range and its tracking, parameter estimation, outlier detection, quality control, and bookkeeping.

4.4 Determination of multi-tone group delay

If the lander signal has other narrow-band tones than the carrier, the multi-tone group delay is determined. For instance, Chang'E3 has 4 primary and 12 secondary side tones with frequencies in range of ± 19.75 MHz with respect to the nominal carrier frequency 8470 MHz that can be used for data analysis (See Figure 3(left)).

We represent the inverse Fourier transform the cross-spectrum of time series of the side-band tone j at the nominal circular frequency $\omega_0+\Delta\omega_j$ in the same form as in Eq. 2, and process then in a similar way as the main carrier, but we do not estimate coefficients b_i, $\dot{\tau}_p$ and $\ddot{\tau}_p$, keeping them fixed to the values determined from processing the signal carrier. We will adjust only the corrections to frequencies $\Delta\omega_j$ and phase delays τ_{pj} for each side-band tone using least squares.

The array of phase delays τ_{pj} and their uncertainties determined from the scatter of processed visibilities, as well as the phase delay of the signal carrier, are used for the evaluation of the multi-tone group delay τ_{mg} and multi-tone phase delay τ_{mp} using weighted least squares with weights set to be reciprocal to phase delay uncertainties:

$$\omega_j \tau_{pj} = \omega_0 \tau_{mp} + (\omega_j - \omega_0)\tau_{mg}. \quad (3)$$

Since the group delay precision is reciprocal to the spanned bandwidth, the precision of a multi-band group delay is better than the precision of a broad-band group delay. The bandwidth of Chang'E3 broadband signal is $\sim$2 MHz and spanned bandwidth of side-band tones is 39.5 MHz.

We will develop new software to implement these steps of the data analysis pipeline. That will include a search for suitable side-band tones, computation of τ_{pj}, evaluation of their uncertainties, outlier detection, quality control, bookkeeping, and computation of the multi-band group delay.

4.5 Forming phase delay differences

After the best estimates of phase and group delays from the lander are computed, differential phase and group delays between observations of calibrators and the lander are calculated. First, the contributions of source structure to phase and group delays of calibrators $\tau_{\rm str}$ are computed for given observations using the 2D Fourier transform of their brightness distribution (Charlot, 1990). This contribution accounts for the deviation of the source brightness distribution from the δ-function. These contributions are subtracted from delays computed during fringe fitting. Then time series of phase delays, phase delay rates and group delays of a calibrator are expanded into the basis spline functions with smoothing constraints, and group and phase delays of calibrators are interpolated to the middle epochs of scans of lander observations (See Figure 5).

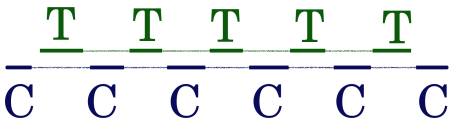

Figure 5: Illustration of phase referencing observations. The array observes the target (T) then slews to a calibrator (C). The cycle is repeated. Fringe phases of the target and the calibrator are shown with a thick line. They are interpolated (thin lines), and the phase differences are computed for a number of common epochs.

The time series of differential phase and group delays are produced by differencing data from the calibrator and the lander referred to the common epoch and common frequency. These differential phase and group delays form the basis for further analysis.

We will develop new software for the interpolation of phase and group delays of calibrators sources and computation of differential phase and group delays. We will incorporate existing open source image radio reconstruction software DifMAP (Shepherd, 1997) into the data analysis pipeline.

4.6 Reconstruction of the lander radio image

Visibility phase has a 2π ambiguity. Since phase delay is proportional to phase, it inherits 2π ambiguity. Ambiguities in differential phase delays have to be resolved before their in data processing, i.e. an integer number N that makes the total phase $\varphi + N \cdot 2\pi$ has to be found. This is

a critical part of the analysis. The feasibility of resolving phase delay ambiguity depends on the signal spectrum, signal strength, and the experiment design. A general approach is to use group delay as a starting point with imposing constraints. A differential group delay from the broad-spectrum lander signal constituent (See right plot in Figure 3) is unambiguous. The multi-tone group delays of a lander have ambiguities that are reciprocal to the minimum frequency difference between tones. Since multi-tone group delay ambiguity spacings are large (15.6 μs or 4.7 km for Chang'E3), broad-band group delays are precise enough to resolve these ambiguities. If the accuracy of the broad-band or multi-tone delays is better than 1/6 of the ambiguity spacing that is reciprocal to the carrier frequency (118 ps or 3.5 cm for Chang'E3), then ambiguities are resolved easily. In other cases additional information should be used to provide constraints.

We will run the self-calibration image reconstruction procedure adopted in radioastronomy (Thompson et al., 2017; Petrov, 2021). The true lander image is expected to be a δ-function. The phase noise in the data and sparseness of observations will cause a deviation of the reconstructed image from δ-function, and spurious peaks will appear. Inaccuracies in the a priori lander position will cause a residual motion of the lander with respect to the calibrator, which will smear the image. Figure 6 shows an initial image of AGN J1458+1427 that was observed in one scan with a 5-station VLBA sub-network using 60 second integration time as an illustration of how a raw lander radio-image recovered from VLBI data may look.

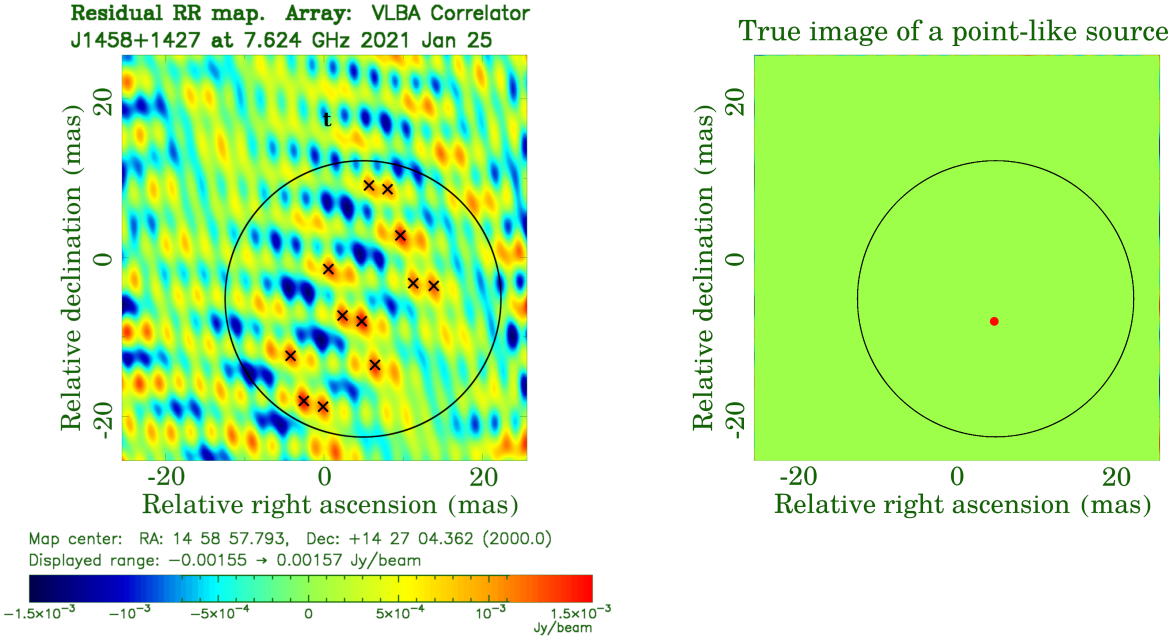

Figure 6: *Left:* Example of our work for image reconstruction from VLBI observations of point-like AGN J1458-1427. Due to hardware malfunction a number of observing stations had phase instability similar to what we expect in lander image because of its residual motion. Sign × shows maxima that are image artifacts due to smearing. *Right:* True image of a point-like source.

The reconstructed image has a number of local maxima, one of them is located at the lander position. The previous adjustment of the lander position limited the number of maxima to consider. A black line in Figure 6 shows the errors ellipse inferred from position adjustments for illustrative purposes. The maxima above some level with respect to the main maximum are shown with × sign. A coordinate of each point on an image is tied to the calibrator position

that is taken from the catalogue of absolute AGN positions derived from analysis of numerous programs of absolute astrometry for last 25 years (Beasley et al., 2002; Fomalont et al., 2003; Petrov et al., 2005, 2006; Kovalev et al., 2007; Petrov et al., 2008; Condon et al., 2017; Petrov and Taylor, 2011; Schinzel et al., 2015, 2017; Fey and Charlot, 1997; Petrov et al., 2011a,b; Petrov, 2011, 2012, 2013; Gordon et al., 2016; Shu et al., 2017; Petrov et al., 2019; Popkov et al., 2021; Petrov, 2021). The algorithm checks all maxima, and executes the following procedure for each maximum. First, it determines the right ascension and declination of the maxima in the inertial coordinate system from the image. Second, it adjusts the lander position in the selenocentric coordinate system. Third, it computes the theoretic path delay using the adjusted position for all observations. Fourth, it forms the residuals between the computed path delays and the observed differential phase and group delays and between the computed path delay rates and the observed path delay rates. Fifth, the algorithm finds a set of N admissible integer ambiguities for each observable at a given baseline and a given scan. Parameter N can vary in a range of 2 to 10 depending on data quality. Sixth, the algorithm computes the statistics of the residuals for each set of admissible ambiguities. When phase delay ambiguities are resolved correctly, the differential phase delay residuals have zero mean and the standard deviation that is consistent with the noise in data and residual atmospheric fluctuations. When phase delay ambiguities are resolved incorrectly, differential phase delay residuals are biased and have an excessive scatter. The algorithm evaluates the probability of a false selection of the integer ambiguity based on the statistics of the residuals. All maxima at the image are examined, and that maximum that provides the minimum of the probability of the false phase delay ambiguity among all admissible maxima is selected. **As a results of this process, ambiguity-free estimates of phase delay and improved estimates of lander position are computed.** The improved lander position is used for re-computation of differential phase delays and re-imaging the lander. Then the procedure is repeated. The iterations are stopped when convergence is reached.

We expect that the image quality from Lunar lander observations will be better than in Figure 6, but our algorithm will converge to a solution even with such a poor image. Indeed, imaging the lander dramatically reduces the number of admissible combinations of integer ambiguities.

We will develop software for implementation of the above algorithm. We will develop software that examines probability of false ambiguity resolution, computes uncertainties of phase and group delays, evaluates position of the lander, and checks convergence.

4.7 Analysis of differential phase delays

The time series of differential phase delays $\Delta\tau_p$, phase delay rates $\Delta\dot{\tau}_p$, and phase delay accelerations $\Delta\ddot{\tau}_p$ are used for a final estimation of lander position using least squares. Then adjustments of the lander position, phase delay ambiguities, as well as parameters of the signal carrier frequency jitter b_i are used as a priori for the last round of data analysis of the original visibility data with applied outliers flagging. Inaccuracy in the a priori lander position result in a residual motion of the lander. That residual motion is eliminated in the final round of data analysis.

We will develop software for computation of the final position of the lander and its position offset with respect to calibrator sources. We will develop software that will write the results into database files in VGOSDB format adopted by the International VLBI Service for Geodesy and Astrometry and put there a) time series of estimates of phase delays, phase delay rates, phase accelerations, and group delays; b) time series of lander angular position

offsets with respect to calibrator sources; and c) auxiliary information about VLBI observations that is present in VGOSDB databases.

5 Proposed work

We aim to develop a semi-automated tool PlaVDA that would ingest the correlator output of VLBI observations of a lander and extragalactic sources that can be considered as a Level 1 data product. It will compute observables that are suitable for scientific analysis in depth: time series of differential phase delays, phase delay rates and group delays, as well as updated lander position as a by-product. These observables can be treated as a Level 2 data product, and they will become an input for the community to make a combined analysis of VLBI and LLR observations for adjustments of parameters of Lunar tides, improvement of the Moon orbit and other quantities using existing tools such as Geodyn (John et al., 2015) and GINS. Both packages have already been used for processing VLBI data in the past by various analyses groups and thus, only a minimal effort is required to adapt the software to process data output from PlaVDA. **Scientific analysis of Level 2 data that includes a refinement of Lunar rotation parameters, improvement of the Moon's orbit, improvement of parameters of the Moon's interior that describes tides, is beyond the scope of the proposed work, but the tool that we will develop will make it possible.**

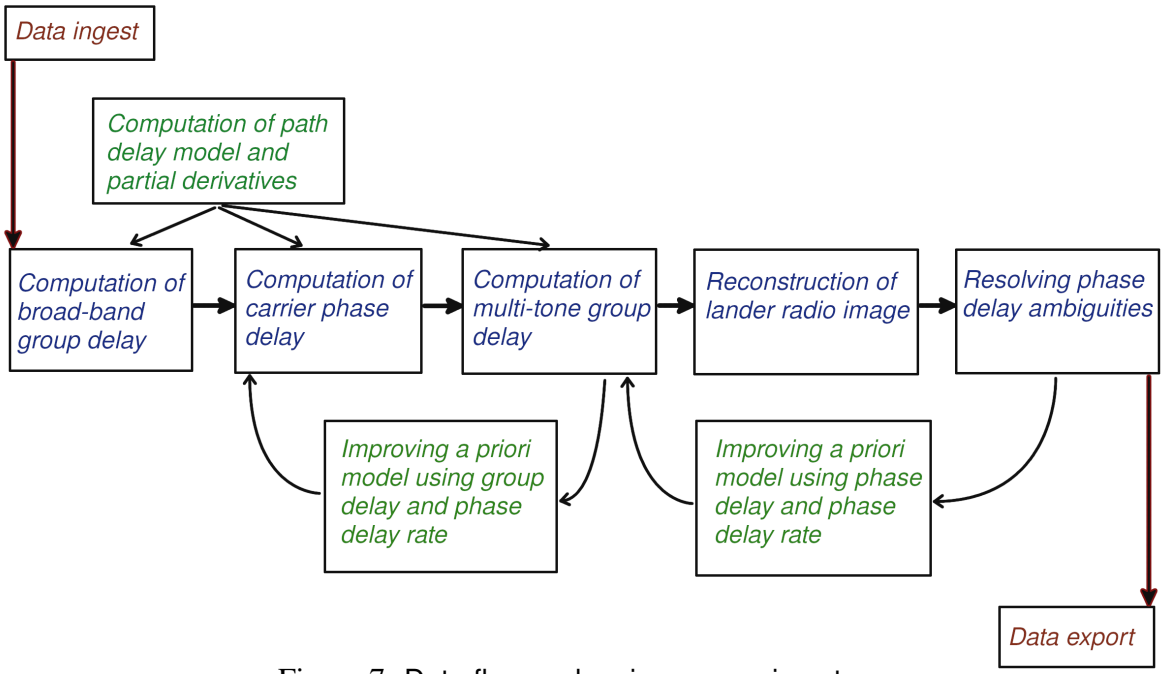

Figure 7: Data flow and major processing steps

We will use existing open source tools of VLBI data analysis, specifically, VLBI Time Delay (VTD) library for computation of path delay for extragalactic sources, PIMA — a general purpose fringe fitting software, and DifMAP — a general purpose differential VLBI image software and adapt them for solving the problem of producing ambiguity-free differential phase and group delays. We will be following the coding practice we adhered in our prior work for development of analysis of VLBI observations of AGNs. PlaVDA will execute all the steps described above. Specifically, we will develop algorithms and implement them in software for

- computation of VLBI path delay of an object on the Moon or other body in the Solar System;
- estimation of position of an object on the Moon or other body in the Solar System using path delay;
- evaluation of phase delay from a carrier and side-band tones of an object with residual motion such as a Lunar lander;
- resolving phase delay ambiguities guided by analysis of local maxima in a lander radio image;
- quality control of each step that includes detection of outliers, their flagging, estimation of the probability of a false detection and a false integer ambiguity value.

We will develop the pipeline software that will combine existing analysis programs and those that we will develop for processing Lunar lander data in one package PlaVDA. It will take the initial cross-correlation data and generate the output database file in VGOSDB format with analysis results. PlaVDA will accept a plain ascii control file in a format `keyword: value` that describes all steps of the data analysis pipeline (See Figures 7 and 8). To stay within the budget, we adopt a guided semi-automatic data analysis approach. That means that a PlaVDA control file in part will be created manually and in part by PlaVDA. PlaVDA will have a command line interface in a form `plavda task -c control_file -r run_level -v verbosity` where `task` is one of analyze, visualize, update. Qualifier `run_level` determines the step of the pipeline to be executed or a combination of steps, including `all` for running the entire analysis job in a totally automatic fashion.

```
Observation description section
  keyword: value
  ...
Analysis description section
  Run_level: name
    Keyword: value
    ...
  Run_level: name
    Keyword: value
    ...
    @{include_file_name}
Output description section
    Keyword: value
    ...
```

Figure 8: PlaVDA control file template. Clause `@{include_file_name}` forces PlaVDA to read the contents of that file and then continue.

At the very beginning, task `update` will create an initial control file using a template. A user will execute the pipeline step by step augmenting `run_level`. PlaVDA will write intermediate results on disk, as well as new sections of the PlaVDA control file that will can be used for further analysis. For instance, PlaVDA will analyze autocorrelations and determine automatically the list of frequencies side-tones. It will generate autocorrelation plots. A user will examine autocorrelation plots using task `visualize` and either confirm the selection or edit that list.

Then running PlaVDA with task `update` will incorporate the edited list of side-band frequencies in the control file.

A user will amend the control file during the course of analysis. By the end of the guided run, a full control file will be created. That file will allow a user to run PlaVDA in a totally automatic fashion using option `run_level all`. The control file will have an option to automatically submit Level 2 resulting dataset to Crustal Dynamics Data Information System (CDDIS)[1]. The adopted approach will allow to reproduce results.

5.1 Validation

We will be using two experiments from the OCEL campaign (Observing the Chang'E3 Lander with VLBI) run in 2015–2016 (Haas et al., 2017) for validation of PlaVDA package. These data are publicly available at CDDIS[2] hosted at NASA. Huang et al. (2014); Han et al. (2019a,b); Klopotek et al. (2019) performed analysis of group delays and reached position accuracy 3–10 meters. These results demonstrate that the data are high quality. The experiment included a number of blocks of phase referencing observations. The authors of the cited papers did not make an attempt to work with phase delays and did not provide publicly accessible tools. We will go beyond of what Han et al. (2019a); Klopotek et al. (2019) have achieved, process phase delays, and make the tools and results of our analysis publicly available.

Fully successful analysis of phase referencing VLBI lander observations is expected to provide a significantly better position accuracy, below 10 cm, which is significant improvement with respect to the accuracy achieved from processing group delays. In order to validate differential phases, we will analyze the time series in instantaneous position offsets from existing OCEL VLBI data will. In particular, we will compute the root mean square of the time series and establish the presence or absence of a systematic pattern in the residuals.

5.2 Data management

The input Level 1 data that we will be using for validation are archived at the CDDIS together with all other VLBI data for space geodesy. The CDDIS provides tools for data ingest, search, performs backup, and provides an access to format descriptions[3]. The CDDIS mission is to keep the data for the scientific community indefinitely. Future VLBI Lunar lander observations will be archived as CDDIS.

The output of processing Level 1 data in a form suitable for planetary data analysis, Level 2 data, will be deposited to CDDIS using established VGOSDB format (Gipson, 2021) adopted by the geodetic community for archiving *all* Level 2 VLBI geodetic data. Therefore, users that are interested in VLBI data will expect to find lander VLBI data for selenodesy there. A typical size of the Level 2 dataset is 1 Gb.

We will make source code developed in this project publicly available at `https://github.com/NASA-Planetary-Science` under Apache License 2.0.

[1] http://cddis.nasa.gov

[2] See https://cddis.nasa.gov/archive/vlbi/ivsdata/swin/2015/20151201_rd1510_v001_swin.tar.bz2 as an example

[3] See, f.e., VLBI Level 1 format description: https://doi.org/10.5067/VLBI/vlbi_l1a_swin_001

5.3 Prior work

The team has an extensive experience in processing VLBI data for geodetic and astronomical observations. We have developed software VTD, PIMA, pSolve for data analysis of extragalactic sources and processed over 6000 geodetic VLBI experiments and 1000 astronomy observations (Petrov and Ma, 2003; Petrov et al., 2009, 2011b; Petrov, 2007; Krásná and Petrov, 2021). We have extensive experience in imaging active galactic nuclei from VLBI observations (Petrov et al., 2011a; Petrov, 2021). We ran a preliminary analysis of VLBI experiments from the OCEL campaign (Haas et al., 2017; Klopotek et al., 2017, 2019) and familiarized ourselves with these data.

5.4 Risk mitigation

Resolving phase delay ambiguities always brings a risk of a failure. Feasibility of phase delay resolution depends on the level of unaccounted errors: if there are systematic errors that are a substantial fraction of the ambiguity spacing, for instance due to instrumental errors in VLBI hardware, then ambiguity resolution may not be feasible. Our approach with estimation of the probability of a false ambiguity resolution is designed to detect such a situation and provide a measure of the phase delay scatter. If the phase delay scatter is low, and therefore, phase delay ambiguity resolution is feasible, there is a risk that the initial lander position based on group delay may be biased. Our approach to generate a lander image and run the ambiguity resolution procedure using local maxima on the image as an initial value will mitigate the risk.

5.5 Future observations

Our validation plan is based on publicly available observations and does not depend on other observations. At the same time, the National Radio Astronomical Observatory has awarded to our team observing time with the Very Long Baseline Array for observations of Lunar Node-1 Payload on the Intuitive Machines NOVA-C Lander (LN-1) in 2022. This opportunity to collect new data and analyze them provides us an additional motivation to develop PlaVDA tool and emphasizes the timeliness of the project. LN-1 does not bring an instrument payload designed for VLBI — we will be observing the telemetry signal. With an expectations of many space vehicles be landing on the Moon within this decade, an opportunity emerges to perform selenodesy observations **almost for free**, provided planetary scientists have a tool for processing these data.

6 Deliverables and Outcomes

In a course of the project we will

- develop software tool PlaVDA for processing Level 1 VLBI observations of a Lunar lander. The tool will compute group delays, phase delay, and phase delay rates at a range of epochs and generate Level 2 product in VGOSDB format. We will make the source code of that tool publicly available at `https://github.com/NASA-Planetary-Science`.
- process two publicly available VLBI experiments of observing Chang'E3 lander and submit Level 2 data product at CDDIS in PY3.
- validate Level 2 data product using Geodyn and GINS software.
- prepare a NASA Technical Memorandum with a detailed algorithm description.
- submit a paper to Advanced in Space Research that describes PlaVDA and results of Level 2 validation.

7 Management plan and milestones

The chart below shows the schedule for implementing the tasks. The schedule is arranged to give an approximately uniform deployment of effort for the team.

Table 1: Schedule chart

Activity name	PY1	PY2	PY3
Development of algorithms for processing group delays	•		
Development of algorithms for processing phase delays	•	•	
Processing existing VLBI data and the tool validation		•	•
Writing papers and reports			•

The Principal Investigator, Leonid Petrov, geophysicist in Geodesy & Geophysics Laboratory (Code 61A) at NASA GSFC will manage the project. He will coordinate the efforts of the team. Leonid Petrov will develop algorithms, design the software tool, and work on implementing the algorithms into software together with the software developer. He will design the test suite. The PI is responsible for submission of PlaVDA source code to Github depository and for submission to CDDIS of the Level 2 data products derived by processing of archival Level 1 data from VLBI observations of Chang'E3 lander.

The co-I Vishnu Viswanathan, will set up the interface between the PlaVDA tool and GINS software to enable the ingestion, testing and validation of Level-2 data, such as time series of differential phase delays, phase delay rates, group delay, lander position with GINS. He will will perform a cross-validation of the lander position estimate using a combination of two independent datasets: Level-2 VLBI data and LLR data, enabling the quantification of the augmentation of LLR data using VLBI.

The co-I Frank Lemoine, geophysicist NASA GSFC Code 61A, will perform validation of the PlaVDA results of processing VLBI observations of Chang'E3 using Geodyn.

The software developer, TBD, will work with the PI on coding PlaVDA and preforming tests.

The collaborator Erwan Mazarico, geophysicist of NASA GSFC, Code 698 will consult the team on the models of the Moon libration and providing the most up-to-date Moon ephemerides.

The collaborator Jean-Charles Marty, CNES, will consult the team on GINS software and provide assistance on establishing the interface between the PlaVDA tool and GINS software.

The collaborator Frederic Jaron will implement the near-field VLBI delay model in DiFX correlator and contribute to the development of the software for correcting visibilities for imperfections in the correlator model based on his prior publication.

The collaborator Rüdiger Haas, the principal investigator of VLBI OCEL campaign, will consult the team about details of these observations.

All teams members will be contributing in writing a technical memorandum and the journal paper.

8 References

Beasley, A. J., D. Gordon, A. B. Peck, L. Petrov, D. S. MacMillan, E. B. Fomalont, and C. Ma (2002), "The VLBA Calibrator Survey-VCS1." *Astrophys. J. Suppl. Ser.*, 141, 13–21 doi: 10.1086/339806.

Bender, P. L., D. G. Currie, S. K. Poultney, C. O. Alley, R. H. Dicke, D. T. Wilkinson, D. H. Eckhardt, J. E. Faller, W. M. Kaula, J. D. Mulholland, H. H. Plotkin, E. C. Silverberg, and J. G. Williams (1973), "The lunar laser ranging experiment." *Science*, 182, 229–238 doi: 10.1126/science.182.4109.229.

Chapront, J., M. Chapront-Touzé, and G. Francou (2002), "A new determination of lunar orbital parameters, precession constant and tidal acceleration from LLR measurements." *Astronomy & Astrophysics*, 387, 700–709 doi: 10.1051/0004-6361:20020420.

Charlot, P. (1990), "Radio-source structure in astrometric and geodetic very long baseline interferometry." *Astron. J.*, 99, 1309–1326 doi: 10.1086/115419.

Condon, J. J., J. Darling, Y. Y. Kovalev, and L. Petrov (2017), "A Nearly Naked Supermassive Black Hole." *Astrophys. J.*, 834, 184 doi: 10.3847/1538-4357/834/2/184.

Counselman, III, C. C., H. F. Hinteregger, R. W. King, and I. I. Shapiro (1973), "Precision Selenodesy via Differential Interferometry." *Science*, 181, 772–774 doi: 10.1126/science.181.4101.772.

Currie, Douglas, Simone Dell'Agnello, and Giovanni Delle Monache (2011), "A lunar laser ranging retroreflector array for the 21st century." *Acta Astronautica*, 68, 667–680 doi: 10.1016/j.actaastro.2010.09.001.

Deller, A. T., W. F. Brisken, C. J. Phillips, J. Morgan, W. Alef, R. Cappallo, E. Middelberg, J. Romney, H. Rottmann, S. J. Tingay, and R. Wayth (2011), "DiFX-2: A More Flexible, Efficient, Robust, and Powerful Software Correlator." *Publ. Astron. Soc. Pacific*, 123, 275 doi: 10.1086/658907.

Deller, A. T., W. M. Goss, W. F. Brisken, S. Chatterjee, J. M. Cordes, G. H. Janssen, Y. Y. Kovalev, T. J. W. Lazio, L. Petrov, B. W. Stappers, and A. Lyne (2019), "Microarcsecond VLBI Pulsar Astrometry with PSRπ II. Parallax Distances for 57 Pulsars." *Astrophys. J.*, 875, 100 doi: 10.3847/1538-4357/ab11c7.

Deller, A. T., S. J. Tingay, M. Bailes, and C. West (2007), "DiFX: A Software Correlator for Very Long Baseline Interferometry Using Multiprocessor Computing Environments." *Publ. Astron. Soc. Pacific*, 119, 318–336 doi: 10.1086/513572.

Dickey, J. O., P. L. Bender, J. E. Faller, X X Newhall, R. L. Ricklefs, J. G. Ries, P. J. Shelus, C. Veillet, A. L. Whipple, J. R. Wiant, J. G. Williams, and C. F. Yoder (1994), "Lunar laser ranging: A continuing legacy of the apollo program." *Science*, 265, 482–490 doi: 10.1126/science.265.5171.482.

Duev, D. A., G. Molera Calvés, S. V. Pogrebenko, L. I. Gurvits, G. Cimó, and T. Bocanegra Bahamon (2012), "Spacecraft VLBI and doppler tracking: algorithms and implementation." *Astronomy & Astrophysics*, 541, A43 doi: 10.1051/0004-6361/201218885.

Dumberry, Mathieu and Mark A. Wieczorek (2016), "The forced precession of the moon's inner core." *Journal of Geophysical Research: Planets*, 121, 1264–1292 doi: 10.1002/2015je004986.

Fey, Alan L. and Patrick Charlot (1997), "VLBA Observations of Radio Reference Frame Sources. II. Astrometric Suitability Based on Observed Structure." *Astrophys. J. Suppl. Ser.*, 111, 95–142 doi: 10.1086/313017.

Folkner, W. M., P. Charlot, M. H. Finger, J. G. Williams, O. J. Sovers, Xx Newhall, and Jr. Standish, E. M. (1994), "Determination of the extragalactic-planetary frame tie from joint analysis of radio interferometric and lunar laser ranging measurements." *Astron. & Astrophys.*, 287, 279–289.

Fomalont, E., T. Martin-Mur, J. Border, C. Naudet, G. Lanyi, J. Romney, V. Dhawan, and B. Geldzahler (2010), "Spacecraft navigation using the VLBA." In *10th European VLBI Network Symposium and EVN Users Meeting: VLBI and the New Generation of Radio Arrays*, vol. 10, 66.

Fomalont, E. B., L. Petrov, D. S. MacMillan, D. Gordon, and C. Ma (2003), "The Second VLBA Calibrator Survey: VCS2." *Astron. J.*, 126, 2562–2566 doi: 10.1086/378712.

Gipson, John (2021), "vgosdb manual." Technical report, IVS, URL https://ivscc.gsfc.nasa.gov/IVS_AC/vgosDB/vgosDB_format_2021Sep20.pdf.

Gordon, D., C. Jacobs, A. Beasley, A. Peck, R. Gaume, P. Charlot, A. Fey, C. Ma, O. Titov, and D. Boboltz (2016), "Second Epoch VLBA Calibrator Survey Observations: VCS-II." *Astron. J.*, 151, 154 doi: 10.3847/0004-6256/151/6/154.

Haas, R., S. Halsig, S. Han, A. Iddink, F. Jaron, L. La Porta, J. Lovell, A. Neidhardt, A. Nothnagel, C. Plötz, G. Tang, and Z. Zhang (2017), "Observing the Chang'E3 Lander with VLBI (OCEL)." In *Proceedings of the First International Workshop on VLBI Observations of Near-field Targets*, vol. 1, 41–64, URL http://www3.mpifr-bonn.mpg.de/div/meetings/vonft/pdf-files/Proceedings2017.pdf.

Han, Songtao, Axel Nothnagel, Zhongkai Zhang, Rüdiger Haas, and Qiang Zhang (2019a), "Fringe fitting and group delay determination for geodetic VLBI observations of DOR tones." *Advances in Space Research*, 63, 1754–1767 doi: 10.1016/j.asr.2018.11.018.

Han, SongTao, ZhongKai Zhang, Jing Sun, JianFeng Cao, Lue Chen, Weitao Lu, and WenXiao Li (2019b), "Lunar radiometric measurement based on observing china chang'e-3 lander with VLBI—first insight." *Advances in Astronomy*, 2019, 1–10 doi: 10.1155/2019/7018620.

Harada, Yuji, Sander Goossens, Koji Matsumoto, Jianguo Yan, Jinsong Ping, Hirotomo Noda, and Junichi Haruyama (2016), "The deep lunar interior with a low-viscosity zone: Revised constraints from recent geodetic parameters on the tidal response of the moon." *Icarus*, 276, 96–101 doi: 10.1016/j.icarus.2016.04.021.

He, Qing-bao, Qing-hui Liu, Sheng-qi Chang, and Xin Zheng (2017), "A New Try of Connecting Phase and Solving Phase Delay in VLBI." *Chin. Astron. and Astrophys.*, 41, 614–625 doi: 10.1016/j.chinastron.2017.11.011.

Hofmann, F and J Müller (2018), "Relativistic tests with lunar laser ranging." *Classical and Quantum Gravity*, 35, 035015 doi: 10.1088/1361-6382/aa8f7a.

Huang, Yong, Shengqi Chang, Peijia Li, Xiaogong Hu, Guangli Wang, Qinghui Liu, Weimin Zheng, and Min Fan (2014), "Orbit determination of chang'e-3 and positioning of the lander and the rover." *Chinese Science Bulletin*, 59, 3858–3867 doi: 10.1007/s11434-014-0542-9.

James, Nick, Ricard Abello, Marco Lanucara, Mattia Mercolino, and Roberto Maddè (2009), "Implementation of an ESA delta-DOR capability." *Acta Astronautica*, 64, 1041–1049 doi: 10.1016/j.actaastro.2009.01.005.

Jaron, Frédéric and Axel Nothnagel (2018), "Modeling the VLBI delay for earth satellites." *Journal of Geodesy*, 93, 953–961 doi: 10.1007/s00190-018-1217-0.

John, McCarthy, Rowton Shelly, Moore Denise, Pavlis Despina E., Luthcke Scott B., and Tsaoussi Lucia S. (2015), "Geodyn systems description volume 1." Technical report, NASA GSFC, URL https://space-geodesy.nasa.gov/techniques/tools/GEODYN/geodyn_vol1.pdf.

Jones, Dayton L., William M. Folkner, Robert A. Jacobson, Christopher S. Jacobs, Jonathan Romney, and Vivek Dhawan (2020), "Very Long Baseline Array Astrometry of Cassini: The Final Epochs and an Improved Orbit of Saturn." *Astron. J.*, 159, 72 doi: 10.3847/1538-3881/ab5f5d.

Kikuchi, Fuyuhiko, Yusuke Kono, Makoto Yoshikawa, Mamoru Sekido, Masafumi Ohnishi, Yasuhiro Murata, Jinsong Ping, Qinghui Liu, Koji Matsumoto, Kazuyoshi Asari, Seiitsu Tsuruta, Hideo Hanada, and Nobuyuki Kawano (2004), "VLBI observation of narrow bandwidth signals from the spacecraft." *Earth, Planets and Space*, 56, 1041–1047 doi: 10.1186/bf03352546.

Klopotek, Grzegorz, Thomas Hobiger, and Rüdiger Haas (2017), "Geodetic VLBI with an artificial radio source on the moon: a simulation study." *Journal of Geodesy*, 92, 457–469 doi: 10.1007/s00190-017-1072-4, URL https://doi.org/10.1007/s00190-017-1072-4.

Klopotek, Grzegorz, Thomas Hobiger, Ruediger Haas, Frederic Jaron, Laura La Porta, Axel Nothnagel, Zhongkai Zhang, Songtao Han, Alexander Neidhardt, and Christian Ploetz (2019), "Position determination of the chan-e3 lander with geodetic vlbi." *Earth, Planets and Space*, 71, 23 doi: 10.1186/s40623-019-1001-2.

Kopeikin, Sergei M. and Gerhard Schäfer (1999), "Lorentz covariant theory of light propagation in gravitational fields of arbitrary-moving bodies." *Physical Review D*, 60 doi: 10.1103/physrevd.60.124002.

Kovalev, Y. Y., L. Petrov, E. B. Fomalont, and D. Gordon (2007), "The Fifth VLBA Calibrator Survey: VCS5." *Astron. J.*, 133, 1236–1242 doi: 10.1086/511157.

Krásná, Hana and Leonid Petrov (2021), "The use of astronomy VLBA campaign MOJAVE for geodesy." *Journal of Geodesy*, 95 doi: 10.1007/s00190-021-01551-3.

Liu, Shanhong, Jianguo Yan, Qingbao He, Jianfeng Cao, Mao Ye, and Jean-Pierre Barriot (2020), "Precise positioning of chang'e 3 lander based on helmert-VCE-aided weighting method using phase delay data from chinese VLBI network." *Advances in Space Research*, 66, 1485–1494 doi: 10.1016/j.asr.2020.05.034.

Martí-Vidal, I., E. Ros, M. A. Pérez-Torres, J. C. Guirado, S. Jiménez-Monferrer, and J. M. Marcaide (2010), "Coherence loss in phase-referenced VLBI observations." *Astron. & Astrophys.*, 515, A53 doi: 10.1051/0004-6361/201014203.

Matsumoto, Koji, Ryuhei Yamada, Fuyuhiko Kikuchi, Shunichi Kamata, Yoshiaki Ishihara, Takahiro Iwata, Hideo Hanada, and Sho Sasaki (2015), "Internal structure of the moon inferred from apollo seismic data and selenodetic data from GRAIL and LLR." *Geophysical Research Letters*, 42, 7351–7358 doi: 10.1002/2015gl065335.

Matsuyama, Isamu, Francis Nimmo, James T. Keane, Ngai H. Chan, G. Jeffrey Taylor, Mark A. Wieczorek, Walter S. Kiefer, and James G. Williams (2016), "GRAIL, LLR, and LOLA constraints on the interior structure of the moon." *Geophysical Research Letters*, 43, 8365–8375 doi: 10.1002/2016gl069952.

Meyer, Jennifer and Jack Wisdom (2011), "Precession of the lunar core." *Icarus*, 211, 921–924 doi: 10.1016/j.icarus.2010.09.016.

Murphy, T W (2013), "Lunar laser ranging: the millimeter challenge." *Reports on Progress in Physics*, 76, 076901 doi: 10.1088/0034-4885/76/7/076901.

Murphy, T W, E G Adelberger, J B R Battat, C D Hoyle, N H Johnson, R J McMillan, C W Stubbs, and H E Swanson (2012), "APOLLO: millimeter lunar laser ranging." *Classical and Quantum Gravity*, 29, 184005 doi: 10.1088/0264-9381/29/18/184005.

Park, Ryan S., William M. Folkner, Dayton L. Jones, James S. Border, Alexander S. Konopliv, Tomas J. Martin-Mur, Vivek Dhawan, Ed Fomalont, and Jonathan D. Romney (2015), "Very Long Baseline Array Astrometric Observations of Mars Orbiters." *Astron. J.*, 150, 121 doi: 10.1088/0004-6256/150/4/121.

Pavlov, Dmitry (2020), "Role of lunar laser ranging in realization of terrestrial, lunar, and ephemeris reference frames." *Journal of Geodesy*, 94, 5 doi: 10.1007/s00190-019-01333-y.

Pavlov, Dmitry A., James G. Williams, and Vladimir V. Suvorkin (2016), "Determining parameters of moon's orbital and rotational motion from LLR observations using GRAIL and IERS-recommended models." *Celestial Mechanics and Dynamical Astronomy*, 126, 61–88 doi: 10.1007/s10569-016-9712-1.

Petrov, L. (2007), "The empirical Earth rotation model from VLBI observations." *Astron. & Astrophys.*, 467, 359–369 doi: 10.1051/0004-6361:20065091.

Petrov, L. (2011), "The Catalog of Positions of Optically Bright Extragalactic Radio Sources OBRS-1." *Astron. J.*, 142, 105 doi: 10.1088/0004-6256/142/4/105.

Petrov, L. (2012), "The EVN Galactic Plane Survey - EGaPS." *Mon. Not. Roy. Astr. Soc.*, 419, 1097–1106 doi: 10.1111/j.1365-2966.2011.19765.x.

Petrov, L. (2013), "The Catalog of Positions of Optically Bright Extragalactic Radio Sources OBRS-2." *Astron. J.*, 146, 5 doi: 10.1088/0004-6256/146/1/5.

Petrov, L., D. Gordon, J. Gipson, D. MacMillan, C. Ma, E. Fomalont, R. C. Walker, and C. Carabajal (2009), "Precise geodesy with the Very Long Baseline Array." *Journal of Geodesy*, 83, 859–876 doi: 10.1007/s00190-009-0304-7.

Petrov, L., Y. Y. Kovalev, E. B. Fomalont, and D. Gordon (2005), "The Third VLBA Calibrator Survey: VCS3." *Astron. J.*, 129, 1163–1170 doi: 10.1086/426920.

Petrov, L., Y. Y. Kovalev, E. B. Fomalont, and D. Gordon (2006), "The Fourth VLBA Calibrator Survey: VCS4." *Astron. J.*, 131, 1872–1879 doi: 10.1086/499947.

Petrov, L., Y. Y. Kovalev, E. B. Fomalont, and D. Gordon (2008), "The Sixth VLBA Calibrator Survey: VCS6." *Astron. J.*, 136, 580–585 doi: 10.1088/0004-6256/136/2/580.

Petrov, L., Y. Y. Kovalev, E. B. Fomalont, and D. Gordon (2011a), "The Very Long Baseline Array Galactic Plane Survey–VGaPS." *Astron. J.*, 142, 35 doi: 10.1088/0004-6256/142/2/35.

Petrov, L., C. Phillips, A. Bertarini, T. Murphy, and E. M. Sadler (2011b), "The LBA Calibrator Survey of southern compact extragalactic radio sources - LCS1." *Mon. Not. Roy. Astr. Soc.*, 414, 2528–2539 doi: 10.1111/j.1365-2966.2011.18570.x.

Petrov, L. and G. B. Taylor (2011), "Precise Absolute Astrometry from the VLBA Imaging and Polarimetry Survey at 5 GHz." *Astron. J.*, 142, 89 doi: 10.1088/0004-6256/142/3/89.

Petrov, Leonid (2021), "The Wide-field VLBA Calibrator Survey: WFCS." *Astron. J.*, 161, 14 doi: 10.3847/1538-3881/abc4e1.

Petrov, Leonid, Alet de Witt, Elaine M. Sadler, Chris Phillips, and Shinji Horiuchi (2019), "The Second LBA Calibrator Survey of southern compact extragalactic radio sources - LCS2." *Mon. Not. Roy. Astr. Soc.*, 485, 88–101 doi: 10.1093/mnras/stz242.

Petrov, Leonid and Chopo Ma (2003), "Study of harmonic site position variations determined by very long baseline interferometry." *Journal of Geophysical Research: Solid Earth*, 108 doi: 10.1029/2002jb001801, URL https://doi.org/10.1029/2002jb001801.

Popkov, A. V., Y. Y. Kovalev, L. Y. Petrov, and Yu. A. Kovalev (2021), "Parsec-scale Properties of Steep- and Flat-spectrum Extragalactic Radio Sources from a VLBA Survey of a Complete North Polar Cap Sample." *Astron. J.*, 161, 88 doi: 10.3847/1538-3881/abd18c.

Reid, M. J. and M. Honma (2014), "Microarcsecond Radio Astrometry." *Ann. Rev. of Astron. & Astrophys.*, 52, 339–372 doi: 10.1146/annurev-astro-081913-040006.

Schinzel, F. K., L. Petrov, G. B. Taylor, and P. G. Edwards (2017), "Radio Follow-up on All Unassociated Gamma-Ray Sources from the Third Fermi Large Area Telescope Source Catalog." *Astrophys. J.*, 838, 139 doi: 10.3847/1538-4357/aa6439.

Schinzel, F. K., L. Petrov, G. B. Taylor, E. K. Mahony, P. G. Edwards, and Y. Y. Kovalev (2015), "New Associations of Gamma-Ray Sources from the Fermi Second Source Catalog." *Astrophys. J. Suppl. Ser.*, 217, 4 doi: 10.1088/0067-0049/217/1/4.

Shepherd, M. C. (1997), "Difmap: an Interactive Program for Synthesis Imaging." In *Astronomical Data Analysis Software and Systems VI* (G. Hunt and H. E. Payne, eds.), vol. 125 of *Astronomical Society of the Pacific Conference Series*, 77, San Francisco: ASP.

Shu, F., L. Petrov, W. Jiang, B. Xia, T. Jiang, Y. Cui, K. Takefuji, J. McCallum, J. Lovell, S.-o. Yi, L. Hao, W. Yang, H. Zhang, Z. Chen, and J. Li (2017), "VLBI Ecliptic Plane Survey: VEPS-1." *Astrophys. J. Suppl. Ser.*, 230, 13 doi: 10.3847/1538-4365/aa71a3.

Sun, Jing, Geshi Tang, Fengchun Shu, Xie Li, Shushi Liu, Jianfeng Cao, Andreas Hellerschmied, Johannes Böhm, Lucia McCallum, Jamie McCallum, Jim Lovell, Rüdiger Haas, Alexander Neidhardt, Weitao Lu, Songtao Han, Tianpeng Ren, Lue Chen, Mei Wang, and Jinsong Ping (2018), "VLBI observations to the APOD satellite." *Advances in Space Research*, 61, 823–829 doi: 10.1016/j.asr.2017.10.046.

Thompson, A. R., J. M. Moran, and G. W. Swenson, Jr. (2017), *Interferometry and Synthesis in Radio Astronomy, 3rd Edition*. Springer.

Turyshev, Slava G., James G. Williams, William M. Folkner, Gary M. Gutt, Richard T. Baran, Randall C. Hein, Ruwan P. Somawardhana, John A. Lipa, and Suwen Wang (2012), "Corner-cube retro-reflector instrument for advanced lunar laser ranging." *Experimental Astronomy*, 36, 105–135 doi: 10.1007/s10686-012-9324-z.

Viswanathan, V., N. Rambaux, A. Fienga, J. Laskar, and M. Gastineau (2019), "Observational constraint on the radius and oblateness of the lunar core-mantle boundary." *Geophysical Research Letters*, 46, 7295–7303 doi: 10.1029/2019gl082677.

Williams, James G. and Dale. H. Boggs (2015), "Tides on the moon: Theory and determination of dissipation." *Journal of Geophysical Research: Planets*, 120, 689–724 doi: 10.1002/2014je004755.

Williams, James G. and Dale H. Boggs (2016), "Secular tidal changes in lunar orbit and earth rotation." *Celestial Mechanics and Dynamical Astronomy*, 126, 89–129 doi: 10.1007/s10569-016-9702-3.

Williams, James G., Dale H. Boggs, Charles F. Yoder, J. Todd Ratcliff, and Jean O. Dickey (2001), "Lunar rotational dissipation in solid body and molten core." *Journal of Geophysical Research: Planets*, 106, 27933–27968 doi: 10.1029/2000je001396, URL https://doi.org/10.1029/2000je001396.

Williams, James G, Slava G Turyshev, and Dale H Boggs (2012), "Lunar laser ranging tests of the equivalence principle." *Classical and Quantum Gravity*, 29, 184004 doi: 10.1088/0264-9381/29/18/184004.

Williams, James G, Slava G Turyshev, and Dale H Boggs (2014), "The past and present earth-moon system: the speed of light stays steady as tides evolve." *Planetary Science*, 3 doi: 10.1186/s13535-014-0002-5.

9 Biographical Sketches

Leonid Petrov (PI)

Present position:

Geophysicist at NASA GSFC in Geodesy & Geophysics Laboratory at NASA GSFC, VLBI Lead Scientist.

Professional experience:

Since 1988 Leonid Petrov has been working in data analysis of space geodesy and remote sensing data, development of data processing algorithms with the highest accuracy, systems and tools aimed to improvement of the terrestrial and celestial reference frames and Earth orientation parameters. He has developed algorithms and implemented them into software for VLBI scheduling, VLBI post-correlation processing based on cross-spectrum, for computation of theoretical VLBI delay, and for geodetic and astrometric VLBI data analysis based on group delays. He has processed all publicly available VLBI observations suitable for astrometry and geodesy.

Leonid Petrov NASA worked at Goddard Earth Sciences Data and Information Services Center for support of the infrastructure for visualization, analyzing, and access of vast amounts of Earth science remote sensing data. During his carrier has has developed over one million line of code for various scientific applications.

Leonid Petrov has been working on development of advanced methods for processing space geodesy, remote sensing data, and numerical models. He has been working on development and maintenance of the pipeline for prepossessing, analysis, and interpretation of VLBI geodetic experiments that was adopted by the International VLBI Service. He also worked on development and maintenance of the International Mass Loading Service, the International Path Delay Service, the Atmospheric Angular Momentum Service, and the Network Earth Rotation Service.

Management experience:

Managed twenty nine projects under various astronomy programs at the National Radio Astronomy Observatory, the European VLBI Network, Australian National Telescope Facility, East Asian VLBI Network, National Astronomical Observatory of Japan, Korea Astronomy and Space Science.

Managed seven projects under NASA Earth Surface and Interior program and one project under NASA Global Navigation Satellite System Remote Sensing Science Team as a principal investigator.

Education:

Ph.D. of Russian Academy of Sciences, 1995, Astronomy
M.S. of Leningrad National University, 1988, Astronomy

Selected publications

1. **Petrov, L.**, "The wide-field VLBA calibrator survey – WFCS", (2021), Astronomical Journal, 161(1), 15 (25pp). doi: 10.3847/1538-3881/abc4e1

2. **Petrov, L.**, (2016), "The International Mass Loading Service", International Association of Geodesy Symposia, Springer, vol 146, 79–83. doi: 10.1007/1345_2015_218

3. **Petrov, L.**, T. Natusch, S. Weston, J. McCallum, S. Ellingsen, S. Gulyaev, (2015). "First scientific VLBI observations using New Zealand 30 meter radio telescope WARK30M", Publications of the Astronomical Society of the Pacific, 127, 516–522

4. **Petrov, L.**, (2015), Modeling of path delay in the neutral atmosphere: a paradigm shift, to appear in the Proceedings of the 12th European VLBI Network Symposium and Users Meeting, 7-10 October 2014 Cagliari, Italy http://arxiv.org/abs/1502.06678

5. P. Sarti, C. Abbondanza, **L. Petrov**, M. Negusini, (2010) "Effect of antenna gravity deformations on VLBI estimates of site positions", Jour. of Geodesy, DOI: 10.1007/s00190-010-0410-6.

6. **Petrov, L.**, D. Gordon, J. Gipson, D. MacMillan, C. Ma, E. Fomalont, R. C. Walker, C. Carabajal, (2009) "Precise geodesy with the Very Long Baseline Array", Journal of Geodesy, vol. 83(9), 859.

7. **Petrov, L.**, (2007) "The empirical Earth rotation model from VLBI observations", Astronomy and Astrophysics, vol. 467, p. 359.

8. **Petrov, L.**, C. Phillips, A. Bertarini, A. Deller, S. Pogrebenko, A. Mujunen, (2009) "The use of the Long Baseline Array in Australia for precise geodesy and absolute astrometry", Publications of the Astronomical Society of Australia, 26(1), 75-84.

9. **Petrov, L.**, J.-P. Boy, (2004) "Study of the atmospheric pressure loading signal in VLBI observations", Journal of Geophysical Research, 10.1029/2003JB002500, vol. 109, No. B03405.

10. **Petrov, L.**, C. Ma, (2003) "Study of harmonic site position variations determined by VLBI", Journal of Geophysical Research, vol. 108, No. B4, 2190.

11. **Petrov, L.**, O. Volvach, N. Nesterov, "Measurements of horizontal motion of the station Simeiz using VLBI", (2001) Kinematic and Physics of Celestial Bodies, Vol. 17, N5, p. 424–436.

There are 59 peer reviewed works with a total of 2383 citations. Hirsch index 26.

Vishnu Viswanathan (Co-I)

DR. VISHNU VISWANATHAN
Center for Space Sciences and Technology, University of Maryland, Baltimore County (UMBC)
Planetary Geology, Geophys. and Geochem. Lab, NASA Goddard Space Flight Center (GSFC)
Bldg. 34, S296A, 8800 Greenbelt Rd., Greenbelt, MD, 20771, United States
Email: vishnu.viswanathan@nasa.gov, Tel: +1 301-614-6466, Mob: +1 202-876-6449

EDUCATION

Ph.D., Astronomy &Astrophysics, Paris Observatory (IMCCE/PSL/OCA), France, 2017
M.S., Aero. & Space Sys. Eng., National School of Aero. and Space Eng. (ISAE), France, 2013
B.Tech., Electronics and Communication Eng., National Institute of Tech., Trichy, India, 2011

PROFESSIONAL EXPERIENCE RELATED TO THIS PROPOSAL

Dr. Viswanathan has extensive experience analyzing lunar laser ranging data using GINS software. In 2017, Dr. Viswanathan improved the orbital-rotational dynamical model of the Moon and fitted it to over five decades of lunar laser ranging (LLR) data with gravity field constraints from the NASA GRAIL mission. This model is one of the three primary references in the world that provides high-precision planetary and lunar ephemerides. In 2018, Dr. Viswanathan used this model to perform a fundamental physics test of the universality of free fall using the Earth-Moon system as test bodies, improving upon previous constraints on the principle of equivalence. In 2019, Dr. Viswanathan further expanded the capabilities of this model that resulted in the strongest constraint known for the shape and size of the lunar core-mantle boundary. In 2020, Dr. Viswanathan published two white papers submitted to the Committee on the Planetary Science Decadal Survey (2023-2032) of the NAS/USA, and to the Artemis III SDT, representing the interests, objectives and goals of the global LLR instrument, analysis and observer community.

APPOINTMENTS

2021 – present	Assistant Research Scientist, UMBC/GSFC, USA
2019 – 2021	Post-doctoral Research Associate, UMBC/GSFC, USA
2017 – 2019	Post-doctoral Researcher, Paris Observatory, IMCCE/PSL, France
2014 – 2017	Doctoral Researcher, Géoazur, Nice Observatory, France

RELEVANT PUBLICATIONS

- Ray, R.D., **Viswanathan, V.**, Chao, B.F., "Is there a six-year ocean tide?" (Submitted 08/21)
- **Viswanathan, V.**, et al. 2021. "Extending Science from Lunar Laser Ranging". *BAAS, 53*(4); doi:10.3847/25c2cfeb.3dc2e5e4
- Mazarico, E., and 20 co-authors, incl. **Viswanathan, V.** 2020, "First Two-way Laser Ranging to a Lunar Orbiter: infra-red observations from the Grasse station to LRO's retro-reflector array". *EPS* 72, *113*; doi:10.1186/s40623-020-01243-w
- **Viswanathan, V.**, Rambaux, N., Fienga, A., Laskar, J., Gastineau, M. 2019, "Observational Constraint on the Radius and Oblateness of the Lunar Core-Mantle Boundary". *GRL* 46, 7295–7303; doi:10.1029/2019GL082677
- **Viswanathan, V.**, Fienga, A., Minazzoli, O., Bernus, L., Manche, H., Laskar, J., Gastineau, M. 2018, "The new lunar ephemerides INPOP17a and its application to fundamental physics". *MNRAS* 476, *1877–1888*; doi:10.1093/mnras/sty096
- Courde, C., and 10 co-authors, incl. **Viswanathan, V**. 2017, "Lunar laser ranging in infrared at the Grasse laser station". *A&A.* 602, *A90*; doi:10.1051/0004-6361/201628590

Frank Lemoine (Co-I)

https://science.gsfc.nasa.gov/sed/bio/frank.g.lemoine

NASA Goddard Space Flight Center — Frank.G.Lemoine@nasa.gov
Geodesy & Geophysics Laboratory, Code 61A — Tel: (301) 614-6109
Greenbelt, MD 20771 U.S.A. — Fax: (301) 614-6522

CURRENT POSITION: 1995 — present: Geophysicist, NASA GSFC.

RESEARCH AREAS: Satellite geodesy; The determination and maintenance of the terrestrial reference frame; Determination of changes in Mean sea level; Precise orbit determination for artificial satellites; Mapping of the static and time-variable gravity field of the Earth and planets from satellite tracking data; Analysis of laser altimeter data.

EDUCATION:

1984,	B.S.E.	Princeton University.
1986	M.S.	University of Colorado, Boulder.
1992	Ph.D.	University of Colorado, Boulder.

PROFESSIONAL ACTIVITIES

• Project Scientist, NASA Space Geodesy Project (Oct. 2018 – Present).
• Co-I Lunar Orbiter Laser Altimeter, Lunar Reconnaissance Orbiter (2008 – Present).
• Co-chair, POD Team for Jason-2 & Jason-3, 2008 – Present.
• Chair & Member Governing Board, International DORIS Service (IDS), 2017 – 2024.
• Director of GSC DORIS Analysis Center, providing weekly SINEX series, and full reprocessing of DORIS satellite data for ITRF2008, ITRF2014, and ITRF2020.
• Member, Central Bureau, International Laser Ranging Service (ILRS).
• Co-I Gravity Recovery and Interior Laboratory (GRAIL), NASA Discovery mission.

SELECTED PUBLICATIONS

Belli, A., N.P. Zelensky, **F.G. Lemoine**, and D.S. Chinn. (2021). "Impact of Jason-2/T2L2 Ultra-Stable-Oscillator Frequency Model on DORIS stations coordinates and Earth Orientation Parameters." *Adv. Space Res.*, **67 (3):** 930-944 doi:10.1016/j.asr.2020.11.034.

Lemoine, F. G. (2020). "The Role of SLR: Science from Satellite Laser Ranging." *International Laser Ranging Service (ILRS) 2016-2019 Report edited by C. Noll and M. Pearlman, NASA/TP-20205008530, NASA Goddard Space Flight Center, Greenbelt, MD, USA, 2020 (https://ilrs.gsfc.nasa.gov/docs/2020/ilrsreport_2016_section2.pdf)*

Pearlman, M.R., C. E. Noll, E.C. Pavlis, **F.G. Lemoine**, et al**.** (2019**).** "The ILRS: approaching 20 years and planning for the future." J. Geodesy, doi:10.1007/s00190-019-01241-1.

Lemoine, F.G., D.S. Chinn, N.P. Zelensky, et al. (2016), "The development of the GSFC DORIS Contribution to ITRF2014," *Adv. Space Res*., doi:10.1016/j.asr.2015.12.043.

Genova, A., S. Goossens, **F.G. Lemoine**, et al. (2015), "Long-term variability of CO2 and O in the Mars upper atmosphere from MRO radio science data," *J. Geophys. Res.-Planets, 120(5), 849–868*, doi: 10.1002/2014JE004770.

Lemoine, F.G., S. Goossens, T.J. Sabaka, et al. (2014), "GRGM900C: A degree 900 lunar gravity model from GRAIL primary and extended mission data", *Geophys. Res. Lett., 41(10),* 3382-3389, doi:10.1002/2014GL060027.

Lemoine, F.G., S. Goossens, T.J. Sabaka, et al. (2013), "High-degree gravity models from GRAIL primary mission data", *J. Geophys. Res.-Planets, 118(8)*, 1676-1698, doi:10.1002/jgre.20118.

Lemoine, F.G., N.P. Zelensky, D.S. Chinn, et al. (2010), "Towards development of a consistent orbit series for TOPEX, Jason-1, and Jason-2", *Adv. Space Res*, 46(12).

Mazarico, E., **F.G. Lemoine**, S.C. Han and D.E. Smith (2010), "GLGM-3: A degree-150 lunar gravity model from the historical tracking data of NASA Moon orbiters", *J. Geophys. Res-Planets, 115(E05001),* doi: 0.1029/2009JE003472.

10 Summary of Work Effort

TABLE OF WORK EFFORT

Work Efforts to be funded by this proposal						
		Commitment (FTE)				
Name	**Role**	**Y1**	**Y2**	**Y3**	**Y4**	Total
Leonid Petrov	PI	0.15	0.10	0.10	n/a	0.35
Vishnu Viswanathan	Co-I	0.10	0.10	0.10	n/a	0.30
Frank Lemoine	Co-I	0.0	0.10	0.10	n/a	0.20
TBD	Support	0.45	0.30	0.30	n/a	1.05
Total funded work effort		**0.70**	**0.60**	**0.60**	**n/a**	**1.90**
Work Efforts proposed, but NOT to be funded by this proposal						
		Commitment (FTE)				
Name	**Role**	**Y1**	**Y2**	**Y3**	**Y4**	Total
Erwan Mazarico	Collaborator	0.10	0.10	0.10	n/a	0.30
Jean-Charles Marty	Collaborator	0.10	0.10	0.10	n/a	0.30
Frederic Jaron	Collaborator	0.10	0.10	0.10	n/a	0.30
Ruediger Haas	Collaborator	0.10	0.10	0.10	n/a	0.30
Total unfunded work effort		**0.40**	**0.40**	**0.40**	**n/a**	**1.20**
TOTAL Work Efforts proposed (Funded + Unfunded)						
		Commitment (FTE)				
Name	**Role**	**Y1**	**Y2**	**Y3**	**Y4**	Total
Leonid Petrov	PI	0.15	0.10	0.10	n/a	0.35
Vishnu Viswanathan	Co-I	0.10	0.10	0.10	n/a	0.30
Frank Lemoine	Co-I	0.0	0.10	0.10	n/a	0.20
TBD	Support	0.45	0.30	0.30	n/a	1.05
Erwan Mazarico	Collaborator	0.10	0.10	0.10	n/a	0.30
Jean-Charles Marty	Collaborator	0.10	0.10	0.10	n/a	0.30
Frederic Jaron	Collaborator	0.10	0.10	0.10	n/a	0.30
Ruediger Haas	Collaborator	0.10	0.10	0.10	n/a	0.30
Grand Total of work effort		**1.10**	**1.00**	**1.00**	**n/a**	**3.10**

11 Current and pending support

Current and pending support — Principal Investigator Leonid Petrov

Current and Pending Support - Principal Investigator, Leonid Petrov

CURRENT					
Proposal Title	Program	Program Officer	Performance Period	PI/Institution	Commitment (FTE/yr)
Towards mm-level direct ties via integrated GNSS and VLBI interferometric measurements	Global Navigation Satellite System Research	Gerald Bawden	09/20 to 08/23	York, Johnathan / University of Texas	PY1: 0.08, PY2: 0.08, PY3: 0.08

Current					
Proposal Title	Program	Program Officer	Performance Period	PI/Institution	Commitment (FTE/yr)
Mitigation of the impact of antropogenic space-born radio interference on geodetic VLBI infrastructure	Earth Surface and Interior	Ben Phillips	01/21 to 12/22	Habana, Nlingi/ SSAI	PY1: 0.10, PY2: 0.10

Current					
Project	Program	Program Officer	Performance Period	PI/Institution	Commitment (FTE/yr)
Space Geodesy Project	Earth Surface and Interior	Ben Phillips	10/21 to 09/26	NASA GSFC	0.7

Frank G. Lemoine, Co-Investigator

A. Current Support

Title	NASA Space Geodesy Project
Project Scientist	**F.G. Lemoine (NASA)**
Project Manager	S. Merkowitz (NASA GSFC)
Program Manager	Benjamin Phillips (Benjamin.R.Phillips@nasa.gov). Tel. 202-358-5693
Perform. period	ongoing
Commitment	~7.5 person-months/annum

Title	Precise Orbit Determination for TOPEX-Sentinel6A for Climate Data Records.
Project Scientist	**F.G. Lemoine (NASA)**
Project Manager	P. Vaze (NASA/JPL)
Program Manager	Nadya Vinogradova-Shiffer (Nadya.vinogradova-shiffer@nasa.gov) Tel. 202-358-0976
Perform. period	ongoing
Commitment	~1.2 person-months/annum

Activity	Community Service, Associate Editor Journal of Geodesy
Project Scientist	**F.G. Lemoine (NASA)**
Project Manager	n/a
Program Manager	n/a
Perform. period	2020-2024
Commitment	~1.2 person-months/annum

Frank G. Lemoine, Co-Investigator

B Pending Support:

Title	Geodetic Reference Antenna in Space (GRASP)
PI	R.S. Nerem (University of Colorado, Boulder)
Co-Is	**F. Lemoine** (NASA GSFC), S. Luthcke (NASA GSFC), C. Ma (NASA GSFC), et al.
Program	NNH15DA011O-Earth Venture Mission-2 (EVM-2)
Program Manager	
Perform. period	Jan. 1 2017 – Apr. 30, 2024
Funding	Approx. $50-180K/annum, depending on mission phase (GSFC portion)
Commitment	1.0 person months/annum (FY2017-FY2020); 6.5 person months/annum (FY2022-FY2023) 2.0 person months/annum (FY2024)

VISHNU VISWANATHAN, Co-Investigator

Current Support:

Title:	**Combination of LLR and GRAIL to constrain the lunar interior**
Program:	Planetary Geodesy - Internal Scientist Funding Model (ISFM)
Sponsor:	NASA
Point of Contact:	Dr. Robert Fogel, 202-358-2289, rfogel@nasa.gov
Principal Investigator:	Dr. Erwan Mazarico (GSFC)
Period of Performance:	03/2019-03/2022
Commitment:	1.0, 1.0, 0.5 FTE/yr

Title:	**Independent Measurement of Saturn's Dissipation using Cassini Astrometric Data**
Program:	Cassini Data Analysis Program (CDAP)
Sponsor:	NASA
Point of contact:	Dr. Henry Throop, 202-358-3709, HQ-CDAP@mail.nasa.gov
Principal Investigator:	Dr. Vishnu Viswanathan (UMBC/GSFC)
Co-Investigators:	Dr. E. Mazarico (GSFC), A. Liounis (GSFC), Dr. S. Goossens (GSFC), Dr. M. Neveu (UMD/GSFC)
Period of Performance:	03/2021-02/2024
Commitment:	0.30, 0.25, 0.25 FTE/yr

Title:	**Retracing the Reorientation and Tidal History of the Moon**
Program	Planetary Geodesy – Internal Scientist Funding Model (ISFM)
Sponsor	NASA
Point of Contact	Dr. Robert Fogel, 202-358-2289, rfogel@nasa.gov
Principal Investigator	Dr. Vishnu Viswanathan (UMBC/GSFC)
Co-Investigator	Dr. E. Mazarico (GSFC), Dr. S. Goossens (GSFC), Dr. R. H. Tyler (UMBC/GSFC)
Collaboratory	Dr. D. E. Smith (MIT)
Period of Performance	01/2022-12/2022
Commitment:	0.2 FTE/yr

Pending Support:

None.

The current proposal is not listed here, as per the Guidebook for Proposers Responding to a NASA Notice of Funding Opportunity (February 2022).

12 Budget Justification (narrative) including facilities and equipment

12.1 NASA Budget Justification

The page is intentionally left blank.

See the next page.

Title: Augmenting Lunar Laser Ranging observations with Very Long Baseline Interferometry
GSFC PI Name: Leonid Petrov
Submitted in response to NNH21ZDA001N-PDART, Planetary Data Archiving, Restoration, and Tools, C.4

Budget Justification: Narrative and Details

Budget Justification: Narrative

NASA Center Funding
Labor Redacted Costs Only

Per ROSES solicitation instructions, all labor dollars are redacted from budgets in Proposal Documents.
NASA Center Funding By Program Year

	PY 1 Cost	PY 2 Cost	PY 3 Cost	Total Cost
NASA/GSFC	11,416	14,974	19,749	46,139
Total:	11,416	14,974	19,749	46,139

GSFC Civil Servant Roles and Cost Basis:

LEONID PETROV, PI, will coordinate the efforts of the team. Leonid Petrov will develop algorithms, design the software tool, and work on implementing the algorithms into software together with the software developer. He will design the test suite. The PI is responsible for submission of PlaVDA source code to Github depository and for submission to CDDIS of the Level 2 data products derived by processing of archival Level 1 data from VLBI observations of Chang'E3 lander.

FRANK LEMOINE, Co-I, will perform validation of the PlaVDA results of processing VLBI observations of Chang'E3 using Geodyn.

ERWAN MAZARICO, Collaborator, will consult the team on the models of the Moon libration and providing the most up-to-date Moon ephemerides.

The civil servants included in this budget are proposed at the following skill levels:

GSFC Civil Servant Name	Budgeted Skill Title
LEONID PETROV	Scientist-Tier 2
FRANK LEMOINE	Scientist-Tier 3

GSFC proposal budgets are based on four Scientist skill levels with Scientist-Tier 1 reflecting the experience level equivalent to GS-13 and Scientist Tier-4 the experience level of GS-15 Step 8-10.

The cost of the labor (salary and fringe) is based on GSFC's established salary rates for the skill levels shown in the above table. GSFC fringe dollars are based on a percent applied to salary dollars using GSFC established rates per year.

GSFC On-Site/Near-Site Contractor Roles and Cost Basis:

The following on-site contractors are needed. The cost estimates are based on currently established loaded rates for the contracts that already exist at GSFC. However, no separate budget/budget justification is required from on-site/near-site contractors.

TBD, Support, will work with the PI on coding software tool PlaVDA and preforming tests.

Other Direct Costs

GSFC Off-Site Subcontracts / Subaward:

The basis of estimate and detailed budgets for off-site institutions are provided in the Budget Details section below.

Non-US Government Recipient: UMBC
Description of the Work: Dr. Vishnu Viswanathan will provide his expertise in using GINS software for a multi-technique software developed by the French National Center for Space Studies (CNES), to cross-validate the Level-2 data output from the proposed Planetary VLBI Data Analysis (PlaVDA) tool. Co-I Viswanathan will set up an interface between the PlaVDA tool and GINS software to enable the ingestion, testing and validation of Level-2 data (such as time series of differential phase delays, phase delay rates, group delay, lander position) with GINS. GINS software has already been used for processing VLBI data in the past by various analyses groups and thus only a minimal effort is required to adapt the software to process data output from PlaVDA. Co-I Viswanathan will reuse his implementation of the effect of solid tides on the Moon, previously used to process lunar laser ranging observation, and adapt it for enhancing the lander position estimation using the Level-2 data products. The enhancements are expected to minimize residuals and will help assess if phase delay ambiguities and other systematic errors were resolved correctly by PlaVDA. Co-I Viswanathan will perform a cross-validation of the lander position estimate using a combination of two independent datasets: Level-2 VLBI data and LLR data, enabling the quantification of the augmentation of LLR data using VLBI. Dr. ViswanathanБ─≥s previous work on the high-fidelity processing of LLR data will be used and will require only minimal effort to assess the potential of the proposed data validation using the combination. Co-I Viswanathan will assist in supporting the proper archiving of the data produced from the work described and in writing the report and publication of the results.

Reason for subcontracting: Dr. Vishnu Viswanathan posses a unique qualicication that is indispensible for this project. In particular, he has a hands on experience in processing LLR data that is substantiated by his publications. He has an experience with GINS software that will be used at the validation phase of our project.

Materials and Supplies (ie, < $5K per unit; otherwise, see Equipment)
This table reflects GSFC's budget for materials and supplies which to cover cost of replacement of failing computer parts, such as harddrives, power supply units, and for for computer upgrade; consumables suchas printer toner; upgrades of memory, CPU, and storage. Cost estimates are based on recent similar procurements initiated by GSFC or recent quotes from local vendors.

Item	PY 1	PY 2	PY 3	Total
Parts for miscellaneous computer upgrades and consumables	2,000	2,000	0	4,000
Total:	2,000	2,000	0	4,000

Travel

The budget includes travel as shown below based on the following cost assumptions:

- Estimated airfare and auto rental costs were obtained from either NASA's customary source or from other airfare estimating search engines (ie, Travelocity, etc.); also, per diem costs were obtained from http://www.gsa.gov/

- Inflation of 3% per year is applied for annual occurrences.
- Prior to international travel, NASA civil servants are expected to have physical exams and vaccinations. The associated medical costs are treated as research expenses and included, if applicable, under Other costs below.

Cost Details
Trip 1

	Lodging	MI&E or Per Diem	Airfare	Ground Trans	Auto Rental	Conf Fee	Fuel	Parking	Tolls	Other	Total	
Rate	288	79	700	100	0	960	0	0	0	100		
Nbr of People	1	1	1	1								
Nbr of Days	5	5			5							
Total	1,440	395	700	100	0	960	0	0	0	100	0	PY 1
											3,806	PY 2
											0	PY 3
											3,806	Total

Purpose of Trip: Attend the AGU general assembly
Depart From: Washingtono DC
Arrive To: San Francisco, CA

Trip 2

	Lodging	MI&E or Per Diem	Airfare	Ground Trans	Auto Rental	Conf Fee	Fuel	Parking	Tolls	Other	Total	
Rate	279	121	1,400	100	0	620	0	0	0	100		
Nbr of People	1	1	1	1								
Nbr of Days	6	6			6							
Total	1,674	726	1,400	100	0	620	0	0	0	100	0	PY 1
											0	PY 2
											4,901	PY 3
											4,901	Total

Purpose of Trip: To attend the EGU General assembly
Depart From: Washington DC
Arrive To: Vienna, Austria

Summary of Travel Budget Requirements

Domestic/Foreign; Purpose	PY 1	PY 2	PY 3	Total
Domestic; Attend the AGU general assembly	0	3,806	0	3,806
Foreign; To attend the EGU General assembly	0	0	4,901	4,901
Total:	0	3,806	4,901	8,707

Other

Publications – page charges for a paper in Advances of Space Research. Cost estimates are based on quot from
the published adjusted for inflation.

Item	PY 1	PY 2	PY 3	Total
Advances in Space Research	0	0	2,900	2,900
Total:	0	0	2,900	2,900

Other Direct Costs, SED - These costs, as discussed in NASA financial regulations, are for services to support the research effort that go beyond the standard costs considered under Center Engineering, Safety, and Operations (Center Overhead) and are not incurred elsewhere within GSFC. Within the Sciences and Exploration Directorate these costs cover system administration for the complex information technology services required to support the proposed research activities, administrative and resource analysis support, and supplies to support the research effort.

Other Costs, Non-SED Assessments - These costs, as discussed in NASA financial regulations, are for services to support the management and engineering effort that go beyond the standard costs considered under Center Engineering, Safety, and Operations (Center Overhead) and are not incurred elsewhere within GSFC. Within the Flight Projects Directorate, these costs cover system administration for the complex information technology services required to support the proposed project activities, administrative and resource analysis support, and supplies to support the management effort.

Other Costs, Reserves - Program does not requires reserves.

Facilities and Administrative (F&A) Costs, GSFC
NASA CESO (Center Engineering, Safety, and Operations) is managed from Headquarters and is therefore excluded from this proposal.

Cost Sharing/Leveraging/Contributions

Description of Required Facilities and Equipment

Existing Facilities and Equipment for Which Funding is Not Requested

The existing facilities and equipment needed to carry out the proposed research are available at the proposer's institution, NASA/Goddard Space Flight Center. These include a 40-core Xeon computer at the Geodesy & Geophysics Lab, Earth Sciences Division in the
Sciences & Exploration Directorate.

Budget Justification: Details

Below is the total budget for the items described in the Budget Narrative. Also below are any supporting budgets.

Per ROSES solicitation instructions, all labor dollars are redacted from budgets in Proposal Documents.

12.2 UMBC Budget Justification

The page is intentionally left blank.

See the next page.

Co-I Vishnu Viswanathan (UMBC/GSFC) – Statement of Work

Title: Augmenting Lunar Laser Ranging Observations with Very Long Baseline Interferometry
Program: Planetary Data Archiving, Restoration and Tools (NNH21ZDA001N-PDART)

Co-I Viswanathan will provide his expertise in using GINS software – a multi-technique software developed by the French National Center for Space Studies (CNES), to cross-validate the Level-2 data output from the proposed Planetary VLBI Data Analysis (PlaVDA) tool. Co-I Viswanathan will set up an interface between the PlaVDA tool and GINS software to enable the ingestion, testing and validation of Level-2 data (such as time series of differential phase delays, phase delay rates, group delay, lander position) with GINS. GINS software has already been used for processing VLBI data in the past by various analyses groups and thus only a minimal effort is required to adapt the software to process data output from PlaVDA. This work will also be facilitated via the expertise provided by GINS software lead, Collaborator Marty. Co-I Viswanathan will reuse his implementation of the effect of solid tides on the Moon, previously used to process lunar laser ranging observation, and adapt it for enhancing the lander position estimation using the Level-2 data products. The enhancements are expected to minimize residuals and will help assess if phase delay ambiguities and other systematic errors were resolved correctly by PlaVDA. Co-I Viswanathan will perform a cross-validation of the lander position estimate using a combination of two independent datasets: Level-2 VLBI data and LLR data, enabling the quantification of the augmentation of LLR data using VLBI. Dr. Viswanathan's previous work on the high-fidelity processing of LLR data will be used and will require only minimal effort to assess the potential of the proposed data validation using the combination. Co-I Viswanathan will assist in supporting the proper archiving of the data produced from the work described and in writing the report and publication of the results. Co-Viswanathan anticipates spending 0.1 FTE/yr over project years 1, 2 and 3 for the successful completion of the stated tasks.

13 NASA Budget Details (redacted)

The page is intentionally left blank.

See the next page.

Report Created On: 03/04/2022

COMPETITION SENSITIVE - FOR PROPOSAL SUBMISSION & PANEL REVIEW ONLY
Budget by Program Year

Solicitation: NNH21ZDA001N-PDART, Planetary Data Archiving, Restoration, and Tools, C.4
GSFC Proposer Name: Leonid Petrov

Proposal Title: Augmenting Lunar Laser Ranging observations with Very Long Baseline Interferometry

Total Excluding Labor Dollars and Indirect Costs: $46,139
Proposal Start Date: 10/01/2022
Proposal End Date: 09/30/2025

Description	PY 1 FTE	PY 1 Cost	PY 2 FTE	PY 2 Cost	PY 3 FTE	PY 3 Cost	Total FTE	Total Cost
A. Senior / Key Personnel (CS Only)								
Scientist-Tier 3			0.10		0.10		0.20	
Scientist-Tier 2	0.15		0.10		0.10		0.35	
Subtotal	0.15		0.20		0.20		0.55	
B.1.a-c Other Personnel (Civil Servants Not Named as Co-I in Proposal)								
Subtotal								
Subtotal GSFC Civil Servants	0.15		0.20		0.20		0.55	
Other Personnel (Non-Civil Servants)								
B.2a.1 On-Site Contractors / Cooperative Agreements / Consultants	0.45		0.30		0.30		1.05	
B.2a.2 On-Site, Test & Fab Pool								
C. Off-Site Subawards / Subcontracts / Consultants								
[GSFC Funded] UMBC	0.10		0.10		0.10	2,320	0.30	2,320
Subtotal Other Personnel	0.55		0.40		0.40	2,320	1.35	2,320
Subtotal Labor-Redacted Cost	0.70		0.60		0.60	2,320	1.90	2,320
Travel Total				3,806		4,901		8,707
Other Costs								
Materials and Supplies		2,000		2,000				4,000
Publications						2,900		2,900
Other Direct Costs, SED		9,416		9,168		9,628		28,212
Non-SED Assessment		0		0		0		0
Reserves/Contingency		0		0		0		0
Subtotal Other Cost		11,416		11,168		12,528		35,112
Indirect CESO								
Total Labor-Redacted Proposal Costs	0.70	11,416	0.60	14,974	0.60	19,749	1.90	46,139

Summary

	PY 1 FTE	PY 1 Cost	PY 2 FTE	PY 2 Cost	PY 3 FTE	PY 3 Cost	Total FTE	Total Cost
Civil Servant, GSFC	0.15		0.20		0.20		0.55	
Contractor, On-Site	0.45		0.30		0.30		1.05	
Subawards / Off-Site	0.10		0.10		0.10	2,320	0.30	2,320
Other Costs, Direct		11,416		14,974		17,429		43,819
Other Costs, Indirect CESO								
Total Labor-Redacted Proposal Costs	0.70	11,416	0.60	14,974	0.60	19,749	1.90	46,139

Funds Distribution

	PY 1 FTE	PY 1 Cost	PY 2 FTE	PY 2 Cost	PY 3 FTE	PY 3 Cost	Total FTE	Total Cost
Other NASA Centers and JPL								
GSFC	0.70	11,416	0.60	14,974	0.60	19,749	1.90	46,139
Total Labor-Redacted Proposal Costs	0.70	11,416	0.60	14,974	0.60	19,749	1.90	46,139

(Labor Dollars Redacted)

CS Labor Distribution by FY

	FY 2023 FTE		FY 2024 FTE		FY 2025 FTE		FY 2026 FTE	
Civil Servant, GSFC	0.15		0.20		0.20			

14 UMBC Budget Details (redacted)

The page is intentionally left blank.

See the next page.

Proposal Title: **Augmenting Lunar Laser Ranging observations with Very long Baelien Interferometry**

Principal Investigator: **Vishnu Viswanathan (UMBC/CSST)**

Proposal Term: **October 1, 2022 to September 31, 2025**

UMBC Budget	YEAR 1		YEAR 2		YEAR 3		TOTAL
Salaries	FTE	Cal	FTE	Cal	FTE	Cal	
Dr. Vishnu Viswanathan	0.10	1.20	0.10	1.20	0.10	1.20	0
Total Salary	**0.10**	1.20	**0** **0.10**	1.20	**0** **0.10**	1.20	**0** **0**
Other Direct Costs							
Domestic Travel			0		0		2,320 2,320
Total Other Direct Costs			**0**		**0**		**2,320** **2,320**
Total UMBC Costs			**0**		**0**		**2,320** **2,320**